A toolkit for transposon libraries and functional genomics in intestinal Bacteroidales

Authors

Carlos Geert Pieter Voogdt[1,#], Indra Roux[2], Katharina Müller[1, 6], Nicolai Karcher[1], Afonso Martins Bravo[1] , Lajos Kalmar[2], Vallo Varik[1, 7], Jacob Bobonis[1, 8], Georg Zeller [1, 3, 4], Michael Zimmermann[1], Kiran Raosaheb Patil[2, 5], Athanasios Typas[1,#]

Affiliations

[1] Molecular Systems Biology unit, European Molecular Biology Laboratory, Heidelberg, Germany

[2] The Medical Research Council Toxicology Unit, University of Cambridge, Cambridge, UK

[3] Leiden University Center for Infectious Diseases (LUCID), Leiden University Medical Center, Leiden, Netherlands

[4] Center for Microbiome Analyses and Therapeutics (CMAT), Leiden University Medical Center, Leiden, Netherlands

[5] Department of Biochemistry, University of Cambridge, Cambridge, UK

[6] present address: Global Health Institute, School of Life Sciences, École Polytechnique Fédérale de Lausanne (EPFL), Lausanne, Switzerland

[7] present address: Estonian Biofoundry, Institute of Bioengineering, University of Tartu, Tartu, Estonia

[8] present address: Centre for Microbiology and Environmental Systems Science, Division of Microbial Ecology, University of Vienna, Austria

Contacts:

[#]carlos.voogdt@embl.de, athanasios.typas@embl.de

Keywords

genetic libraries, gut microbiome, essential genes, Bacteroidales, transposon mutagenesis

Abstract

Members of the order Bacteroidales include some of the most prevalent and abundant bacterial species in the healthy human gut microbiota. Yet, most of the functions encoded in their genomes remain poorly characterized, limiting our understanding of the different roles they play in the human gut microbiome. Towards addressing this gap, we developed tools and methods for genome-wide transposon mutagenesis in Bacteroidales, including broad-range transposon vectors with several antibiotic selection markers, a dual conjugation-cloning donor strain, and protocols for convenient library generation in liquid media. We then created saturated, barcoded, insertion mutant libraries in the type strains of three key representatives of the main genera within Bacteroidales: *Bacteroides uniformis* (ATCC 8492), *Phocaeicola vulgatus* (ATCC 8482) and *Parabacteroides merdae* (ATCC 43184). Based on the dense transposon insertion profiles and a workflow for comparing essentialomes across species, we identified 275 core essential genes shared across the three species, and 163 species-specific essential genes, some of which could be explained by functional redundancy and alternative metabolic pathways. We further identified essential non-protein coding elements and essential protein domains with known and unknown functions. Finally, using insertion directionality bias, we could map potential toxic modalities in the three genomes, including toxin-antitoxin pairs, mobile elements encoding toxic products and enzymes leading to toxic metabolic intermediates. Overall, the tools, workflows and genome-wide resources reported here expand the experimental repertoire for characterizing genes in key bacteria of the human gut microbiome, and pave the way for the establishment of similar genetic toolkits for other gut bacteria.

Introduction

Advances in sequencing technologies have revealed an unprecedented taxonomic and genomic diversity within microbial ecosystems[1–6]. Yet, this enormous diversity of microbial gene sequences is also highlighting how little we know about their encoded functions. Even in well-studied model organisms, such as *Escherichia coli* and *Bacillus subtilis,* up to a third of their genes remain poorly characterized[7,8]. The knowledge gap is much larger for the many non-model microbes found in diverse ecosystems. High-throughput reverse genetics, which systematically link genes to each other and to phenotypes, offers a powerful strategy to close this gap in microbial gene function annotation[9–14]. However, applying such approaches to non-model microbes requires efficient genome-wide genetic tools.

Random transposon mutagenesis has been used for decades to generate mutant libraries in bacteria. By inserting at random genomic locations, transposons disrupt genes and create loss-of-function mutant libraries without the need for targeted genetic tools. While originally used for forward genetic screens, the declining cost of sequencing and the incorporation of random DNA barcodes into the transposon[15,16], have transformed transposon mutant libraries into powerful resources for systematic genotype-to-phenotype mapping[17–19]. Libraries containing insertion mutants for thousands of genes can be assessed in hundreds of conditions, such as nutrients, xenobiotics or host colonization, to reveal genes important for fitness in specific environments and to infer functional links between genes with similar phenotypic profiles[14,20–22]. Furthermore, high density transposon mutagenesis also enables the assessment of gene essentiality. In dense libraries, genes and other genetic features intolerant to disruptive insertions can be identified as essential, revealing core functions critical for growth and survival[23–25]. Gene essentiality can be context-dependent, changing with the environment and/or genetic background[9,26,27]. Thus, identifying and comparing essential genes across species can both highlight shared central functions and help to understand species-specific physiology.

One of the most extensively studied microbial ecosystems is the human intestinal microbiota. This ecosystem contains 200-500 bacterial species, considerably varying across individuals at the strain-level, and therefore also, at the gene level[28,29]. Since most of these species are phylogenetically distant from classical model bacteria, their genomes contain a large fraction of uncharacterized genes. To expedite their functional interrogation, transposon mutant libraries have been made in several human gut bacterial species, such as *Enterococcus faecalis*[30], *Akkermansia muciniphila*[31], *Clostridioides difficile*[32], *Bifidobacterium breve*[22], *Lactobacillus casei*[33], and several members of the order Bacteroidales[20,21,34–38]. Part of one of the two major phyla found in the human gut microbiome (Bacteroidota), Bacteroidales contain some of the most prevalent and abundant species of the healthy human gut microbiota. These species are mainly part of three genera: *Bacteroides*, *Phocaeicola* and *Parabacteroides*[39], some of which have been associated with health benefits such as the production of short chain fatty acids through fermentation of dietary complex carbohydrates[40–42].

While dense transposon libraries have been generated in Bacteroidales species, these have almost exclusively focused on the *Bacteroides* genus and in particular two of its species, *B. thetaiotomicron* and *B. fragilis*. Many other prevalent and abundant Bacteroidales species of the healthy human gut microbiota remain genetically unexplored. Transposon mutagenesis is well suited to address these gaps, but generating dense libraries across diverse gut Bacteroidales species and strains requires versatile vectors and easy-to-implement methods

100 and analysis pipelines. To meet this need, we developed a set of broad-range, barcoded
101 transposon vectors and a multi-purpose *E. coli* conjugation donor for the generation of high-
102 density barcoded transposon insertion libraries in multiple Bacteroidales species and strains.
103 We used these genetic tools to generate saturated, barcoded libraries in the type strains of
104 three prominent gut species, *B. uniformis*, *Parabacteroides merdae* and *Phocaeicola vulgatus,*
105 representatives of the three main genera within the order. In addition to conventional library
106 construction via outgrowth on solid media, we established a liquid-based protocol, which is
107 considerably easier and more scalable in confined anaerobic workstations. We demonstrated
108 the utility of these dense libraries through comparative analyses that revealed conserved and
109 species-specific essential genes, essential protein domains, and toxic genetic modalities
110 across the three species.

Results

Novel tools for transposon mutagenesis in Bacteroidales

We set out to create a broad-range barcoded transposon vector able to mutagenize multiple species of Bacteroidales with high efficiency. We used the pSAM-bt plasmid[35] as the basis, and changed several of its features. The *B. thetaiotaomicron rpoD* promoter that drives expression of the Himar1-C9 transposase was replaced by the strong constitutive *B. fragilis* phage promoter P_{BfP1E6}, which is active in different *Bacteroides* species[43]. The native *B. thetaiotaomicron* promoter driving *ermG* expression (erythromycin resistance) was replaced by the hybrid *cepA* promoter[44], as this promoter was previously shown to limit insertional bias in *B. thetaiotaomicron* transposon mutagenesis[21]. Further, we removed the transcriptional terminator in the pSAM-bt transposon to avoid polar mutations in operons, where early termination can block transcription of downstream genes. In its place, we inserted a random sequence flanked by BsmBI restriction sites to enable plasmid barcoding through Golden Gate cloning[45,46]. The barcode entry site is flanked by primer binding sites for barcode sequencing (BarSeq[16]). As resistance to erythromycin is common among various species of Bacteroidales[47], we also created vectors in which the transposon encodes *catP* or *tetQ*, instead of *ermG*[48], providing resistance to chloramphenicol or tetracycline, respectively (Fig. 1A, see supplementary file 1 for plasmid features).

High transformation efficiency is necessary for generating diverse collections of barcoded transposon plasmids. The transformation efficiency of pCV006 (*ermG* version) was very low in the widely used *E. coli* S17-1 conjugation donor, but much higher in the *E. coli* cloning strain EC100D*pir*+ (Extended Data Fig. 1A). Therefore, we engineered EC100D*pir*+ to create a dual cloning-conjugation strain[49]. For this, we used phage P1*vir* to transduce the EC100D*pir*+ cloning strain with a P1 lysate from *E. coli* MFD*pir*+[50], in which the RP4 conjugation locus is flanked by neomycin and apramycin resistance genes, allowing for selection in both antibiotics. We also deleted *dapA* from the chromosome to make the conjugation donor auxotrophic for diaminopimelic acid (DAP), providing a counter-selectable marker. The resulting strain, DATC (DAP Auxotroph Transformation Conjugation donor[49]), has useful genomic features for both cloning and conjugation (Fig. 1B). Importantly, it exhibited high transformation efficiency with pCV006, as its EC100D*pir*+ parent (Extended Data Fig. 1A).

We tested the ability of our new transposon vectors and the DATC *E. coli* donor strain to mutagenize a panel of 32 Bacteroidales strains (21 species from 3 genera). We conjugated either the *ermG*, *catP* or *tetQ* versions of the vector into each of the 32 strains (Fig. 1C), after determining their resistance to erythromycin, chloramphenicol, and tetracycline (Extended Data Fig. 1B). We detected substantial transposon insertion mutagenesis in ~72% (23/32) of the tested recipient strains and in representatives of all 3 genera. The few recipient strains for which we failed to detect transconjugants were spread across the phylogenetic tree, indicating that endogenous strain-specific defenses against conjugation or foreign DNA elements were likely the underlying cause, rather than incompatibility of our vector with specific species. Overall, we generated a set of transposon vectors and a dual cloning-conjugation strain that are useful for transposon mutagenesis in a broad range of Bacteroidales species and strains.

Generation of saturated barcoded transposon libraries in three genera

We used our mutagenesis system to generate high-density, barcoded libraries in the type strains of *Bacteroides uniformis* (ATCC 8492), *Phocaeicola vulgatus* (ATCC 8482) and *Parabacteroides merdae* (ATCC 43184). We first sequenced the three strains and obtained

closed, single-contig genome assemblies, which allowed us to confidently map the transposon insertions. Additionally, to facilitate comparability in downstream analyses, all genomes were annotated using the mettannotator suite[51]. To render our libraries amenable for barcoded sequencing (BarSeq[16]) and further library mutliplexing[38], we inserted DNA barcodes of 25 random nucleotides into pCV006 using Golden Gate cloning (Methods), and a four nucleotide, library-specific index in front of the barcode. Following overnight conjugation of the DATC donor carrying the barcoded pCV006 with *B. uniformis*, *P. vulgatus* or *P. merdae* under aerobic conditions (Fig. 2A), we plated the mutant libraries on more than 25 large (145 mm) petri dishes containing Modified Gifu Anaerobic Medium (mGAM) with erythromycin and incubated these until single colonies were detectable. While outgrowth on solid media is a standard step in transposon library construction, it becomes cumbersome in confined anaerobic chambers, since it limits handling and available space. As an alternative, we conducted the outgrowth of the mutant libraries for 25-28 generations in a single bottle containing 100 ml selective mGAM liquid growth medium – this number of generations approximates the growth required for a single cell to form a visible colony. We cryo-preserved both the solid- and liquid-generated libraries, and used a single library aliquot for transposon insertion sequencing (TnSeq)[52] using a 2-step semi random PCR procedure[53] (Methods). To map the transposon insertion sites to the three genomes, we used TnSeeker (Methods), an in-lab developed software that maps raw TnSeq reads onto the assembled genome, and creates a list of mutants for each library with positional, directional, and barcode information (Fig. 2A).

We identified over 340,000 transposon insertion sites in all six libraries (three species, solid or liquid outgrowth), spread evenly across the genome without insertion bias (Fig. 2B). Barcode analysis revealed that some sites were represented by more than one mutant, and after barcode filtering, we retained between 317,144 and 492,747 uniquely mapping barcodes per library (see Methods). No major differences were observed in the abundance of unique barcodes between species or outgrowth procedure (liquid vs. solid) and across all libraries, with the median number of barcodes per gene being between 54 and 82, and 75% of genes having at least 19 unique barcodes (Extended Data Fig. 2A). Multiple unique barcodes per gene represent independent mutants for this gene, and provide multiple biological replicates in BarSeq experiments, increasing the statistical power for assessing gene fitness[16].

Further characterization of the libraries showed that more than 90% of insertions occurred at TA dinucleotides, as expected for Himar Mariner transposases (Extended Data Fig. 2B), and that the proportion of TA sites with insertions was similar across intragenic, intergenic and annotated non-protein-coding elements, indicating no apparent bias among different genomic elements (Extended Data Fig. 2C). Our libraries also exhibited high insertion saturation, with an average of 76% of genes across the six libraries having more than 75% of their TA sites disrupted by a transposon (Fig. 2C). In line with previous reports on *B. thetaiotaomicron*[21], we observed no directional bias in the *B. uniformis* and *P. merdae* libraries and only a very slight bias in the *P. vulgatus* libraries towards insertions in the sense strand of the targeted gene (Fig. 2D). This suggests that the P_{cepA}-*ermG* promoter-gene combination is well-suited to generate libraries in Bacteroidales species with little to no overall directional bias.

To assess whether the liquid outgrowth protocol affected the library composition, we compared the relative abundances of disrupted genes between liquid- and solid- generated libraries in the three species, approximating gene abundance by the mean read count of its mutants. Although differences between the libraries were observed (see also essentiality analysis later),

mostly for genes with low read counts, the Pearson correlation coefficients were high in all three species (0.66-0.90; Fig. 2E). Thus, as outgrowth in liquid media did not compromise library diversity or introduce systematic bias, we suggest that this liquid protocol can serve as a robust, easy, and cost-effective alternative for generating libraries in gut microbes.

Conservation and species-specificity of gene essentiality in Bacteroidales

We used our transposon libraries to systematically map and compare gene essentiality across *B. uniformis*, *P. vulgatus* and *P. merdae*. The saturation of our libraries made them ideal for predicting gene essentiality with high confidence. We analyzed the TnSeq data using the software package TRANSIT to identify essential genes via a Hidden Markov Model (HMM) and a Bayesian/Gumbel model[54]. To arrive at a single essentiality call per gene, we first consolidated high confidence calls from the HMM and Gumbel methods per library (Extended Data Fig. 3A) and then further consolidated these between the liquid and solid libraries (Extended Data Fig. 3B&C). All essentiality data, including the HMM and Gumbel output, of the three species is provided in supplementary table 1.

About 9% of the coding genes in each of the three species were classified as essential (Fig. 3A). This proportion is similar to previous findings in other Bacteroidales, including *B. thetaiotaomicron* (6.7%[35] and 7.9%[21]) and *Bacteroides fragilis* (12.7%[37]). Similar ranges have been reported in model bacteria, such as *E. coli* (8.3%[25]), *Bacillus subtilis* (6.1%[10]), *Caulobacter crescentus* (12.2%[24]), and several Enterobacteriaceae species (6–9.1%[55]). Importantly, for most genes the essentiality calls agreed between solid and liquid libraries (Extended Data Fig. 3D). In *P. merdae*, *B. uniformis* and *P. vulgatus*, 11.2%, 3.1% and 7.1% of the essential genes respectively, were flagged as being essential in only the solid or liquid library (Fig. 3A). Most of these differential calls were due to low confidence by the HMM and Gumbel method in one of the libraries (Supplementary Table 1), but in some cases biological reasons may explain the differences. For example, pyrimidine biosynthesis genes in *P. merdae* were essential only on solid media (Extended Data Fig. 3E), possibly because metabolite cross-feeding is limited on agar plates, but can occur in liquid culture, rescuing the auxotrophy of these mutants.

We next investigated the conservation and divergence of gene essentiality among the three species. Genes were grouped into families using the Cluster of Orthologous Groups (COGs) at the Bacteroidia (class) taxonomic level from the EggNOG 5.0 database[56], which yielded 452 families containing at least one essential gene. Among these, 63 families lacked representation from one or two of the species. Such absences could reflect genuine species-specific differences, or alternatively, cases where orthologous genes were assigned to different families. To distinguish between these possibilities, we performed a reciprocal best hit (RBH) analysis of protein BLAST searches among the genes of the 63 families (Methods). This identified 14 genes across different families that were close homologs (E-value < 10^{-20}), which we reassigned accordingly (Supplementary table 2). For example, ribosomal binding factor A (*rbfA*) of *B. uniformis* was grouped in a separate COG than its orthologs in *P. merdae* and *P. vulgatus*, despite all three being essential, consistent with findings for *rbfA* in *E. coli*[25]. After RBH-based reassignment, 438 families contained at least one essential gene. Of these, 275 families included essential genes from all three species, while the remaining 163 showed variable conservation and/or essentiality across species (Fig. 3B). The essentiality calls were robust, as similar distributions of conserved and variable essential genes where observed when genes were grouped by their PFAM association (Extended Data Fig. 4A).

The majority of essential genes are conserved across the three species and including essential genes previously identified in *B. thetaiotaomicron*[21] preserved 196 of the 275 (71%) essential gene families (Extended Data. Fig. 4B). Hence, these core essential genes are likely to be conserved across most Bacteroidales and were enriched in core cellular processes, such as translation, cell division and metabolism, but also included genes of unknown function (Fig. 3C, Extended Data. Fig. 4C, Supplementary table 1). In contrast, only 20 genes were uniquely essential in one species and lacked orthologs in the other two species according to the eggNOG COG assignment and our stringent RBH analysis. More than half of the unique essential genes have poor functional annotations (Supplementary table 1). An example of an annotated unique essential gene is an antitoxin in *B. uniformis* (BACUNI_03224), which is part of a putative RnlA/RnlB toxin-antitoxin system.

Interestingly, the 163 gene families with non-conserved essentiality were enriched in coenzyme transport and metabolism (Fig. 3C), suggesting that essentiality can be bypassed either through redundancy (isoenzymes) or via alternative metabolic routes. An example of the latter involves *nadA*, *nadB* and *nadC*, which were assigned as essential in *P. merdae* and *P. vulgatus*, but not in *B. uniformis* and in *B. thetaiotaomicron* according to a prior study[21] (Fig. 3D). These genes encode enzymes that synthesize nicotinate mononucleotide (NaMN) from aspartate[57], a key precursor in the biosynthesis of the essential cofactors NAD and NADP. Loss-of-function mutations in *nadA-C* cause niacin auxotrophy[58]. However, some bacteria can bypass this requirement through a salvage pathway, in which NaMN is produced from exogenous nicotinic acid, likely present in complex mGAM media, via the enzyme PncB[59]. Indeed, *pcnB* is absent from *P. merdae* and *P. vulgatus*, explaining the essentiality of *nadA–C*, but it is present in both *B. uniformis* and *B. thetaiotaomicron*, rendering the route involving *nadA–C* dispensable (Fig. 3D). To investigate further whether functional redundancy contributes to differences in gene essentiality across species in general, we compared the number of genes per species in conserved versus non-conserved essential gene families. Paralogs resulting from gene duplications are known to buffer against gene essentiality[60]. Consistently, conserved essential families contained fewer genes per species than families in which essentiality was not conserved, suggesting that the differences in number of paralogs may explain several cases of non-conserved essentiality across the three species (Fig. 3E). An example is a putative UDP-glucose-6-dehydrogenase in family 2FMZ9 that is essential in *P. vulgatus*, which has only a single copy of this gene, but is dispensable in *P. merdae* and *B. uniformis*, which have two and three paralogs respectively (Extended Data. Fig. 4D).

In summary, the essentialome in the three Bacteroidales genera is strongly conserved and comprised 825 essential genes from 275 families, amounting to ~80% of all essential genes of the three species combined. Species-specific differences in essentiality primarily reflected functional redundancy through gene duplication and alternative metabolic strategies.

Genes encoding essential protein domains

Having highly saturated transposon libraries we next determined essentiality at the sub-gene level of encoded protein domains, as done previously for *E. coli*[25] and *C. crescentus*[24]. To assign domains, we complemented gene annotations with protein domain predictions obtained from InterProScan[61]. More than half of all genes encoded a single protein domain, while about 15–20% encoded either no domain or two domains in the three species – very few proteins had more than two domains (Fig. 4A). Since several genes lacked any InterPro-

303 annotated domain or their domains covered only a fraction of the full-length protein, we
304 classified unannotated sections and inter-domain sequences as independent "regions" for
305 analysis. We used the HMM method of TRANSIT to predict the essentiality state of each TA
306 site in the updated domain-and-region annotated genome. As expected, the majority of TA
307 sites in domains encoded by essential genes were essential, whereas TA sites in non-
308 essential genes were predominantly marked as non-essential (Fig. 4B). However, in some
309 cases, essential domains or regions (defined as having >80% essential TA sites) were
310 embedded within non-essential genes, ranging from 5 to 31 instances in the *P. vulgatus* solid
311 and liquid libraries, respectively. Conversely, we also identified non-essential domains or
312 regions (<20% essential TA sites) within essential genes, ranging from 2 cases in the *B.*
313 *uniformis* solid library to 20 in the *P. vulgatus* solid library (Supplementary table 3).
314
315 We specifically focused on a subset of genes with more than one protein domain/region (~25%
316 of all genes in each species; Fig. 4A) that contained both essential and non-essential
317 domains/regions predicted with high confidence (Methods). To increase robustness, we
318 required each domain/region to contain at least 10 TA sites, and that domain essentiality calls
319 agreed between the liquid and solid libraries. In this way we identified 30 genes as such
320 'domain-specific essentials' (8 in *P. merdae*, 8 in *B. uniformis,* and 14 in *P. vulgatus*), of which
321 3 overlapped between at least 2 species (Supplementary table 3). Although some of these
322 may be false positives due to sporadic insertions at the termini of an essential gene (see also
323 Discussion), most likely represent genuine examples of protein domain essentiality.
324
325 One such example is DNA polymerase I (*polA*), which exhibited a similar insertion pattern
326 across the three species: the N-terminal 5′→3′ exonuclease domain was essential, while the
327 proofreading (3′→5′ exonuclease) and polymerase domains tolerated insertions (Extended
328 Data Fig. 5A). This finding recapitulates known biology of PolA, as the 5'→3' exonuclease
329 activity is vital for DNA replication by processing RNA primers during Okazaki fragment
330 maturation[62]. In contrast, proofreading and DNA polymerase activities can be also performed
331 by other polymerases (e.g., Pol III and Pol II), and hence are dispensable.
332
333 Another example of domain-specific essentiality comes from an uncharacterized gene family,
334 uniquely present in the Bacteroidota phylum. Members of this family (BACUNI_00679,
335 BVU_3062, PARMER_04194) were identified as domain-specific essential genes in all three
336 species (Extended Data Fig. 5B-C). These genes encode an N-terminal lipoprotein signal
337 peptide, a central domain of unknown function (DUF4296) and a C-terminal small beta-barrel-
338 like domain with a disordered region as predicted by Alphafold[63] (Extended Data Fig. 5D).
339 Essentiality mapping revealed that the DUF4296 is indispensable, whereas the C-terminal
340 portion of the protein tolerated insertions. In all three species, this gene is located downstream
341 of *lspA* (Extended Data Fig. 5C), which encodes an essential lipoprotein signal peptidase. The
342 preserved genomic context and the matched essentiality suggest that *lspA* and the
343 uncharacterized protein, may be functionally related.
344
345 A third example of a domain-specific essential gene is *lpxC*, which was annotated as encoding
346 a multifunctional fusion protein. This gene harbored both essential and non-essential domains
347 in *P. merdae* with a similar domain-specific transposon insertion pattern in *B. uniformis* and *P.*
348 *vulgatus* (Fig. 4C). In the Bacteroidota and many other phyla, this gene appears to be a fusion
349 of *lpxC* (N-terminal, predicted UDP-3-O-acyl-N-acetylglucosamine deacetylase activity
350 involved in lipid A biosynthesis), and *fabZ* (C-terminal, predicted beta-hydroxyacyl-(acyl-

351 carrier-protein) dehydratase activity involved in fatty acid biosynthesis) (Fig. 4D). The
352 structural predictions of these domains match very well with their *E. coli* homologues (Fig. 4E,
353 Extended Data. Fig. 6). In several other phyla, including the Pseudomonadota (formerly
354 Proteobacteria), where most of our knowledge on the function of these genes originates, *lpxC*
355 and *fabZ* occur as separate, distantly located genes (Fig. 4D). Both genes are essential in *E.*
356 *coli*[25] and many other bacteria, and are considered antibiotic targets[64–67]. Interestingly, in *E.*
357 *coli*, pharmacological inhibition of LpxC, leads to drug resistance through mutations in
358 FabZ[68,69] and the two proteins have direct functional links[70]. Hence the fusion of LpxC and
359 FabZ in Bacteroidota and other taxa may facilitate direct functional coordination between their
360 activities. The transposon insertions tolerated in the FabZ domain suggest redundancy in the
361 function of this domain that may be compensated by other proteins. To test this hypothesis,
362 we searched for structural homologues of *E. coli* LpxC (PDB: 4mdt[71]) and FabZ (PDB: 6n3p[72])
363 in the proteomes of *B. uniformis*, *P. merdae* and *P. vulgatus*, using FoldSeek[73]. For LpxC, the
364 fusion protein was the only high-confidence hit. In contrast, FabZ searches retrieved several
365 proteins predicted to be structurally similar, though with lower confidence than the FabZ
366 domain of the fusion protein (Fig. 4F & Extended Data. Fig. 6). The retrieved structural
367 homologs are part of PFAM families, some of which are involved in other steps of fatty acid
368 biosynthesis (e.g., BVU_1026 encodes a FabA-domain protein). One or more of these genes
369 may compensate for loss of FabZ function in the *lpxC–fabZ* fusion transposon mutants.
370
371 In summary, our highly saturated transposon libraries reveal that essentiality is not always
372 uniform across a protein, highlighting conserved cases of domain-specific essentiality, and
373 pinpointing essential domains of unknown function, for future targeted functional investigation.
374
375 **Essentiality of non-coding regions**
376 As transposons also insert in non-coding regions of the genome, we used the TRANSIT-based
377 essentiality calling also for non-protein-coding elements in the three genomes. These
378 elements include transfer RNAs (tRNAs) and other non-coding RNAs (ncRNAs), terminal
379 inverted repeat elements (TIREs) of mobile elements, and intergenic regions, defined as any
380 sequence located between annotated features (gene, tRNA, ncRNA, or TIRE). Many of these
381 non-coding elements are relatively short, leading to unclear essentiality predictions; however,
382 for a substantial fraction, we were able to assess essentiality: between ~25% (TIREs) and
383 above 90% (ncRNAs) across the three species (Fig. 5A, Supplementary table 1).
384
385 Universally conserved non-coding elements, such as various tRNAs, the RNase P ribozyme
386 and the signal recognition particle (SRP) RNA were also essential in the three species.
387 Surprisingly, the transfer-messenger RNA (tmRNA) and its associated protein SmpB were
388 essential in *B. uniformis* and *P. vulgatus*, but fully dispensable in *P. merdae*. The tmRNA–
389 SmpB complex rescues ribosomes that are stalled by degrading the mRNA and recycling the
390 incomplete nascent polypeptides[74]. In *E. coli*, alternative ribosome rescue pathways involving
391 *arfA* and *arfB* allow the cells to survive in the absence of tmRNA–SmpB[75–77]. We could not find
392 sequence or structural homologs of *arfA* or *arfB*, or duplicated copies of tmRNA or *smpB*, in
393 any of the three species. This suggests that *P. merdae* may employ a distinct ribosome rescue
394 mechanism that either does not exist in *B. uniformis* and *P. vulgatus*, or the same mechanism
395 exists in all thee but can only compensate for the loss of tmRNA–SmpB complex in *P. merdae.*
396
397 We also analyzed the essentiality of intergenic regions in *P. merdae* (n=2,322), *B. uniformis*
398 (n=2,514), and *P. vulgatus* (n=2,722). We could assess the essentiality status of 75-91% of

399 the intergenic regions (Fig. 5A), and of those with more than five TA insertion sites (above the
400 25th percentile for intergenic TA site density in all three species), only 11 (*P. merdae*), 16 (*B.*
401 *uniformis*), and 26 (*P. vulgatus*) were classified as essential. In most cases (11, 13, and 17 in
402 *P. merdae*, *B. uniformis*, and *P. vulgatus*, respectively), these essential intergenic regions are
403 located immediately upstream of essential genes (Supplementary table 1), suggesting that the
404 transposon insertion disrupts critical regulatory sequences and interferes with essential gene
405 expression. One notable case is an essential intergenic region conserved in all three species,
406 located between the essential δ subunit of DNA polymerase III and a predicted essential helix-
407 turn-helix (HTH) transcriptional regulator. This region is among the longest and most TA-rich
408 intergenic loci (130, 83, and 93 TA sites in *P. vulgatus*, *B. uniformis* and *P. merdae*
409 respectively) (Fig. 5B), yet we observed only 18 (*P. vulgatus*), 7 (*B. uniformis*) or 10 (*P.*
410 *merdae*) insertions. No protein-coding sequence could be detected within it and thus the
411 scarcity of insertions suggests that it may harbor an elaborate regulatory element or a
412 functional RNA not captured by our current annotation pipeline.
413
414 These findings exemplify the potential of using dense insertion libraries for the identification of
415 conserved and species-specific essential elements beyond protein-coding genes.
416
417 **Insertion directionality bias infers toxic modalities in genomes**
418 Transposon libraries can also provide insights into gene interactions by studying polar
419 effects[78,79]. We designed our transposon without a transcriptional terminator to allow for read-
420 through transcription into downstream genes and avoid polar effects when insertions occur in
421 the sense orientation in operons. However such a design may reduce downstream expression
422 of operon genes in antisense insertions, where the transposon integrates opposite to a gene's
423 orientation, through antisense transcription (Fig. 6A). We assessed insertion directionality bias
424 with a binomial test to identify genes showing significant enrichment of sense or antisense
425 insertions. For each gene, we also calculated a directionality ratio, defined as the fraction of
426 sense insertions over all (sense + antisense) insertions and normalized these ratios across
427 libraries (Extended Data. Fig. 7A) to correct for overall insertion bias (Fig. 2D, Supplementary
428 table 4). All libraries contained a small subset of genes with directionality ratio below 0.2 or
429 above 0.8 (Extended Data Fig. 7A). We called significantly biased genes if they met these
430 thresholds and had an adjusted *p*-value of < 0.01 from the binomial tests in both liquid and
431 solid libraries. Based on these criteria we identified 114, 127 and 82 significantly biased genes
432 in *P. vulgatus*, *B. uniformis* and *P. merdae*, respectively (Supplementary table 4).
433
434 Genes are likely biased because the transposon impacts the expression of neighboring genes.
435 We therefore asked whether genes with significant directionality bias also showed a specific
436 orientation of their immediate neighbors. Mapping the four possible orientations of neighboring
437 genes revealed that nearly all biased genes are followed by a downstream gene oriented in
438 the same direction, and hence likely part of the same operon (Fig. 6B; Supplementary table
439 4). This suggests that bias largely reflects whether transposon insertions enable (ratio > 0.8)
440 or prevent (ratio < 0.2) expression of downstream genes of the same operon. Consistent with
441 this, most of the genes that are downstream of a biased gene with ratio > 0.8 (less antisense
442 insertions) were found to be essential (Fig. 6C). Hence antisense insertions are less well
443 tolerated when the downstream gene is essential, by impairing its expression.
444
445 Conversely, genes with a directionality ratio < 0.2 (few sense insertions) showed a depletion
446 of essential genes downstream (Fig. 6C). In these cases, (higher) expression of the

447 downstream gene, while the upstream gene is disrupted by the transposon, is less well
448 tolerated, pointing to a toxic role for the downstream gene product. Toxic modalities are known
449 to occur in bacterial genomes, often in the form of toxin-antitoxin (TA) systems[78,80]. Across the
450 three species, we identified 28 annotated antitoxins (Methods and Supplementary table 4) of
451 which only 7 (2 in *P. merdae*, 3 in *B. uniformis* and 2 in *P. vulgatus*) were positioned upstream
452 and in the same orientation as another gene, often an annotated toxin. Among these, two
453 (PARMER_02862, BACUNI_04310) showed significant bias against downstream expression
454 (Extended Data Fig. 7B). A third candidate antitoxin, not previously annotated as such, was
455 identified in *B. uniformis* (BACUNI_01541) based on its bias and position upstream of an
456 annotated toxin (Extended Data Fig. 7B). In addition, we found two further cases of similar
457 bias in genes annotated as phage defense factors (Extended Data Fig. 7B), suggesting
458 analogous functions to antitoxins in these defense systems.
459
460 Among the other genes showing insertional bias against expression of downstream neighbors
461 (ratio < 0.2; few sense insertions), we identified at least five metabolic genes (2 in *B. uniformis*,
462 2 in *P. merdae* and 1 in *P. vulgatus*), suggesting that transposon disruption may lead to build-
463 up of toxic metabolic intermediates[81,82]. One such example is *gnd* (6-phosphogluconate
464 dehydrogenase) in *B. uniformis*, for which insertional bias is to potentially avoid expression of
465 the downstream pentose phosphate pathway genes *zwf* (glucose-6-phosphate 1-
466 dehydrogenase) and *pgl* (6-phosphogluconolactonase) (Fig. 6D). This suggests that in the
467 absence of functional Gnd, transposon-driven expression of *zwf* (and *pgl*) may lead to a build-
468 up of toxic 6-phosphate gluconate (6P-gluconate), possibly due to an inability of *B. uniformis*
469 to shuttle 6P-gluconate into the Entner-Doudoroff pathway. A similar pattern was found in *P.*
470 *merdae* (Supplementary table 4), but not in *P. vulgatus* (Fig. 6D). Additional examples include
471 genes involved in inositol glycerophospholipid metabolism in *P. merdae* and *B. uniformis*
472 (genes absent in *P. vulgatus*), and a putative esterase involved in ubiquinone biosynthesis
473 specifically in *P. vulgatus* (Extended Data Fig. 7C). In *B. uniformis* we also found biased
474 insertions in a gene encoding a WYL domain that is upstream of a Lin1244/Lin1753-like N-
475 terminal domain-containing gene. Both genes are predicted to be part of a putative
476 biosynthetic gene cluster of unknown function (Extended Data Fig. 7C).
477
478 Beyond individual genes, we observed that sets of biased genes often co-localized within
479 specific genomic regions in each of the three species (Supplementary table 4). To capture this
480 pattern more systematically, we determined directionality bias across the genome using a
481 sliding window approach. This revealed regions with strong bias against downstream
482 expression which often mapped to mobile genetic elements, such as integrative conjugative
483 elements (ICE) and prophages (Fig. 6E). Within ICEs, several mobilization/transfer genes
484 were significantly biased and we hypothesize that transposon-mediated dysregulation of
485 expression of such genes can lead to cell death or possibly to excision of the ICE element
486 (Extended Data Fig. 8A). Similarly, the prophage BV01 in *P. vulgatus*[83] contained a group of
487 genes towards the end of the prophage with strong insertional bias (Extended Data Fig. 8B).
488 Although many genes in this region are of unknown function, it is plausible that dysregulation
489 of (some of the) downstream gene(s) could lead to prophage excision.
490
491 In summary, transposon directionality bias can be used to identify functional dependencies
492 between gene products and the processes in which they are involved, and to highlight the
493 presence of potentially toxic modalities within genomes.

494 **Discussion**
495 Bacteria in the order Bacteroidales are typically dominant members of the human gut
496 microbiota, with several species implicated in both health and disease[39–41], yet many remain
497 understudied and poorly characterized experimentally. In this work, we developed tools and
498 workflows that enable efficient construction of genome-wide transposon insertion libraries in
499 diverse Bacteroidales species and strains. Using these resources, we generated saturated,
500 barcoded mutant libraries in three key representative genera: *Bacteroides*, *Phocaeicola* and
501 *Parabacteroides*. The tools and workflows presented here, include new broad-range
502 transposon vectors with different selection markers, a dual-purpose cloning and conjugation
503 donor strain, a convenient liquid-based protocol for generating libraries and computational
504 scripts/tools for functional genomics analyses. Together, these innovations can be used to
505 expedite the construction and analysis of barcoded mutant libraries across Bacteroidales
506 species. Moreover, the three libraries established here and available to the community, can
507 themselves serve as basis for large-scale gene-phenotype studies aimed at advancing our
508 functional knowledge of this key group of gut bacteria.
509
510 Our dense transposon insertion libraries in *B. uniformis*, *P. merdae* and *P. vulgatus* enabled
511 us to assess gene essentiality within and across these species. Identifying essential genes is
512 valuable for understanding physiology and evolution[23,26,84], refining genome-scale metabolic
513 models[85], predicting antibiotic sensitivities and novel targets[86], and for engineering purposes
514 such as utilizing auxotrophies[87,88]. Although gene essentiality has been mapped in diverse
515 bacteria, cross-species comparisons are notoriously hard because different metrics and
516 methods often produce false negative and positive calls[89]. To address this, we devised a
517 systematic framework based on available bioinformatic tools, which can be used with
518 additional mariner transposon datasets (as demonstrated here by including data from a *B.*
519 *thetaiotaomicron* library[21]). Most essential gene families were involved in core processes and
520 thus were essential across all three species, but some exhibited species-specific essentiality.
521 We showed that species differences in essentiality often arise from functional redundancy and
522 rerouting via alternative metabolic routes. Families with genes of unknown function were found
523 both among conserved and species-specific essential genes.
524
525 In addition to determining gene essentiality, we mined our TnSeq dataset to systematically
526 investigate essentiality of non-protein-coding regions, protein domains and interactions among
527 neighboring genes using directionality bias. This revealed essential intergenic regions, critical
528 protein domains, and indications for metabolic and mobile genetic element toxicities as a
529 consequence of pathway disruption or mobile element activation. Such findings underscore
530 the utility of dense transposon library TnSeq datasets for diverse functional genomics
531 analyses. Looking ahead, applying similar analyses to new TnSeq datasets in additional
532 species, or re-analyzing existing datasets with improved annotations for protein domains[90],
533 coding and non-coding genes[91] and regulatory elements like promoters and terminators[92,93],
534 may yield deeper insight into the conservation and molecular basis of non-coding and protein-
535 domain essentiality, as well as gene-dysregulation-mediated toxicity.
536
537 Our tools and approaches also have limitations. Although our transposon vector design
538 includes promoters shown to be active across multiple species[21,43,44], some strains did not
539 yield transconjugants. In these cases, low conjugation efficiency is likely due to either cell
540 envelope incompatibilities with the RP4 conjugation machinery[94,95] or more likely due to host
541 defense mechanisms that block incoming foreign DNA, e.g., restriction-modification enzymes.

542 While strain-specific strategies can sometimes overcome these barriers, broader solutions
543 have been developed such as mimicking DNA methylation to avoid restriction-modification in
544 the recipient[96] or using non-RP4 based DNA delivery systems like ICE's[97]. Mariner
545 transposons also have inherent limitations, the most notable being their dependency on TA
546 dinucleotide sites for insertion. This bias reduces their ability to target regions sparse in TA
547 sites. In addition, essential genes cannot be directly studied in transposon library screens, as
548 insertions in these regions are by definition lethal. Complementary approaches such as
549 CRISPR interference (CRISPRi) are better suited for probing essential genes and small
550 elements, such as ncRNAs, and have been adapted for *Bacteroides* species[98,99].
551
552 Overall, there is a pressing need for the expansion of systematic genetic tools and genome-
553 wide resources for gut bacteria, if we are to uncover the function and organization of genes in
554 these non-model organisms. In this work, we provide such tools, analytical frameworks and
555 resources for three key representatives of the human gut microbiota. Similar and
556 complementary resources are vital for many other species and genera. This could be the basis
557 for future large-scale genotype-phenotype mapping experiments to accelerate functional
558 annotation and map genetic networks. As shown in other species[13,14,16,21,22] such efforts can
559 provide a broader knowledge base for gene function discovery and for uncovering species-
560 specific aspects of cell physiology. Collectively such efforts will provide a foundation for deeper
561 understanding of the gut microbiome and open new avenues for its modulation.

562 **Methods and materials**

563 **Bacterial strains, growth conditions and antibiotic sensitivity testing**

564 Bacteroidales strains used in this study are reported in Supplementary table 5. Some strains
565 were isolated from fecal samples from healthy donors at the EMBL. The local Bioethics
566 Internal Advisory Committee approved all experiments involving human stool-derived material.
567 Informed consent was obtained from all donors (BIAC2015-009). All Bacteroidales strains
568 were grown at 37°C on modified Gifu Anaerobic Media (mGAM, Nissui Pharmaceutical;
569 05433) in an anaerobic (12% CO_2, 1.5% H_2, 86.5% N_2) vinyl chamber (Coy Laboratory
570 Products Inc.). mGAM media (solid with 2% agar, or liquid) was placed in the anaerobic
571 chamber to become anoxic 24 hours before use. *Escherichia coli* S17-1, *E. coli* EC100D*pir+*
572 (Lucigen/Epicentre) and *E. coli* DATC were grown on Lysogeny Broth (LB) at 37°C. For *E. coli*
573 DATC, LB was supplemented with 0.3 mM diaminopimelic acid (DAP, Sigma-Aldrich; 33240).
574 Generation of the *E. coli* DATC (available at DSMZ; 116187) conjugation donor strain is
575 described in Bobonis *et al.* 2024[49]. To determine the sensitivity of the 32 Bacteroidales strains
576 to erythromycin (Sigma-Aldrich; E5389), chloramphenicol (Sigma-Aldrich; C0378) and
577 tetracycline (Sigma-Aldrich; 87128), 24-hour cultures (stationary phase) grown in mGAM were
578 diluted in a 96-well plate 1:500 into 100 µl fresh mGAM containing antibiotics (50 µg/ml to 0.78
579 µg/ml by 2-fold serial decrease) and grown at 37°C. Optical density was measured every 30
580 minutes at 578 nm for 48 hours in an Epoch2 plate reader (Agilent) connected to a BioStack
581 plate stacker (Agilent) installed in an anaerobic chamber.

582

583 **Construction of transposon vectors**

584 The transposon vector pCV006 (*ermG*) was constructed using Gibson assembly of different
585 template DNA fragments: pSAM_bt (served as vector backbone, Addgene; 112497), *cepA*
586 hybrid promoter sequence RBF-103[44] (synthesized, Eurofins), P_{BfP1E6} promoter sequence
587 (taken from pWW3864[43], kindly provided by Justin Sonnenburg) and a barcode entry
588 sequence containing two BsmBI recognition sequences (synthesized, Eurofins). Fragments
589 were assembled using NEBuilder HiFi DNA Assembly 2x Mastermix (New England Biolabs
590 (NEB); E2621). The Himar1 C9 transposase gene in pSAM_bt contained a BsmBI recognition
591 sequence, which was removed by making a synonymous nucleotide change (G to A) at
592 position 546 relative to the starting nucleotide of the gene reading frame (A of ATG). After
593 completing plasmid pCV006 we used NEBuilder HiFi DNA Assembly 2x Mastermix to replace
594 the *ermG* gene for *catP* (taken from pGT-Ah7, Addgene; 122574) or *tetQ* (taken from pGT-
595 Ah9, Addgene; 122576)[48] to generate plasmids pCV019 and pCV020, respectively. Plasmids
596 pCV006, pCV019 and pCV020 were verified by whole plasmid sequencing (Eurofins) and are
597 available through Addgene (IDs as follows: pCV006: 232824; pCV019: 232825; pCV020:
598 232826). Annotated plasmid sequence of pCV006 is reported in Supplementary file 1.

599

600 **Barcoding of transposon vectors**

601 One µg of pCV006 was digested with 100 units of Esp3I/BsmBI (Thermo Fisher; ER0451) in
602 Tango buffer (Thermo Fisher Scientific (TFS); BY5) supplemented with freshly prepared DTT
603 (Sigma-Aldrich; D0632, 1 mM final concentration) for 16 hours at 37°C, followed by 20 minutes
604 at 65°C. Linearized plasmid was extracted from 1% agarose gel using the GeneJET Gel
605 Extraction and DNA Cleanup Micro Kit (TFS; K0831). Single stranded DNA oligos containing
606 a four nucleotide index in front of a 25 random nucleotide barcode were purchased from
607 Sigma-Aldrich (cartridge purification) (Supplementary table 6). The single stranded oligo was
608 made double stranded by PCR using a reverse primer in a reaction mixture containing: 100
609 pmol barcoded oligo, 500 pmol primer and 100 µl Q5® High-Fidelity 2X Master Mix (NEB;

610 M0492). PCR program consisted of: 3 minutes at 98°C, 25 cycles of 12 seconds/cycle going
611 from 55°C to 50°C (-0.2°C/cycle) followed by 7 minutes at 72°C. PCR reaction was purified
612 using GeneJET Gel Extraction and DNA Cleanup Micro Kit. The linearized plasmid was
613 barcoded and circularized through Golden Gate cloning in three identical reactions each
614 containing: 80 ng linearized plasmid, 9 ng double stranded barcoded oligo (~5-fold molar
615 excess oligo:plasmid), 1 µl NEBridge® Golden Gate Assembly Kit BsmBI-v2 (NEB; E1602), 2
616 µl T4 ligase buffer (NEB; B0202) and water up to 20 µl total volume. The reaction mixtures
617 were incubated for 3 hours at 42°C, after which the three reactions were pooled and purified
618 using GeneJET Gel Extraction and DNA Cleanup Micro Kit. The barcoded plasmids were
619 electroporated into *E. coli* EC100D*pir*+ TransForMax cells (Biozym; 190065) and expanded
620 by growing cells until saturation at 37°C in 200 ml LB with 100 µg/ml ampicillin (Sigma-Aldrich;
621 A9518). The barcoded plasmid library was extracted from EC100D*pir*+ cells by midi-prep
622 (Zymo Research; D4200) and electroporated into the *E. coli* DATC conjugation donor that was
623 grown at 37°C until saturation in 200 ml LB with 0.3 mM DAP and 100 µg/ml ampicillin. Multiple
624 1 ml single-use cryostocks were preserved at -80°C until use in conjugation experiments with
625 type strains of *B. uniformis*, *P. vulgatus* or *P. merdae*.
626
627 **Whole genome sequencing and genome annotation**
628 Genomic DNA was extracted from Bacteroidales strains isolated at the EMBL and the type
629 strains of *B. uniformis* ATCC 8492, *P. vulgatus* ATCC 8482 and *P. merdae* ATCC 43184
630 (purchased from DSMZ) using the ZymoBiomics DNA miniprep kit (Zymo Research; D4300)
631 and measured for molecular weight size distribution using FEMTO pulse (Agilent). High
632 molecular weight DNA was fragmented using Megaruptor 3.0 (Diagenode) to a final size of
633 15-20 kbps. Sequencing libraries were prepared using the SMRTBell 3.0 kit (Pacific
634 Bioscience) as per the manufacturer's instructions. Libraries were size-selected using AMPure
635 PB beads to remove fragments shorter than 5 kbps. Final library yield and fragment size were
636 assessed, and libraries were pooled equimolarly and sequenced on a PacBio Sequel IIe
637 instrument with 30 hours movie time. Genomes were assembled with Flye[100] version 2.9-
638 b1768. We assigned taxonomic labels using the whole genome sequence and GTDB-tk[101]
639 version 2.1.1. Genome sequences generated in this study have been deposited at the ENA
640 under project number ERP180871. The *P. vulgatus* ATCC 8482 and *P. merdae* ATCC 43184
641 genomes were assembled into single contigs of 5.16 and 4.38 Mbps, respectively. The *B.*
642 *uniformis* ATCC 8492 genome assembled into a chromosome of 4.68 Mbps and an extra
643 chromosomal element of 22.7 kbps. Genomes were annotated using the mettannotator
644 pipeline of the EMBL-EBI[51], which utilizes multiple bioinformatics tools to provide information
645 on various identified genetic elements (Supplementary table 1).
646
647 **Conjugation of transposon vectors to Bacteroidales strains**
648 Bacteroidales recipients and *E. coli* DATC donor carrying pCV006, pCV019 or pCV020 were
649 grown at 37°C from a single colony anaerobically in mGAM (Bacteroidales) or aerobically in
650 LB (DATC, supplemented with 0.3 mM DAP and 100 µg/ml ampicillin) for 16-20 hours.
651 Recipient and donor cultures were diluted 100-fold and 250-fold, respectively, in fresh media
652 and grown for 4 hours in same conditions as overnight cultures. Donor cells were washed
653 twice with LB without ampicillin by centrifuging at 3225 *g* for 5 min at RT. Eight OD600nm units
654 of recipient and one OD unit of donor were collected by centrifuging cultures at 3225 *g* for 5
655 minutes. Pellets were resuspended in 25 µl mGAM, and recipient and donor cells were mixed
656 and placed as 50 µl spots on mGAM agar with 0.3 mM DAP. Cells were left to conjugate for
657 16-20 hours at 37°C under aerobic conditions. Cell mixtures were scraped from agar into 1 ml

658 mGAM and washed twice with mGAM without DAP by centrifugation at 3225 *g* for 5 minutes
659 at room temperature. Pellets were resuspended in 1 ml anoxic mGAM without DAP and left to
660 recover for 1 hour at 37°C in an anaerobic chamber. Recovered cultures were diluted 50-fold
661 and 500-fold in mGAM, and 100 µl was plated on anoxic mGAM agar containing 25 µg/ml
662 erythromycin, chloramphenicol or tetracycline. Forty-eight hours after incubation at 37°C in an
663 anaerobic chamber, colonies were counted.
664
665 **Construction of full-scale mutant libraries with outgrowth in solid or liquid media**
666 Saturated *B. uniformis* ATCC 8492 and *P. vulgatus* ATCC 8492 cultures grown anaerobically
667 at 37°C for 24 hours from a single colony were diluted 1:100 in 10 ml MGAM and grown for 4
668 hours. Three cryovials of *E. coli* DATC carrying barcoded pCV006 were thawed and inoculated
669 in 50 ml LB (supplemented with 0.3 mM DAP and 100 µg/ml ampicillin) and grown for 4 hours
670 at 37°C in aerobic conditions with shaking at 180 rpm. Donor cells were washed twice with LB
671 without ampicillin by centrifuging at 3225 *g* for 5 min. Eight OD600nm units of recipient and
672 one OD unit of donor were collected by centrifuging cultures at 3225 *g* for 5 min at RT. Pellets
673 were resuspended in 100 µl mGAM, and recipient and donor cells were mixed in quadruplets
674 by adding 25 µl donor to 25 µl recipient. Separate mixtures were placed as 50 µl spots on
675 mGAM agar with 0.3 mM DAP. Cells were left to conjugate for 16 hours at 37°C under aerobic
676 conditions. Cell mixtures were scraped from mGAM agar into 4 x 1 ml mGAM and washed
677 twice with mGAM without DAP by centrifugation at 3225 *g* for 2 min at RT. Pellets were
678 resuspended in 4 x 1 ml anoxic mGAM without DAP and left to recover for 1 hour at 37°C in
679 an anaerobic chamber. The four separate cell mixtures were pooled and added to 46 ml
680 mGAM. One ml of this was serially diluted 10-fold and plated on mGAM agar with 25 µg/ml
681 erythromycin and 200 µg/ml gentamicin to determine the input transconjugant CFUs. For the
682 solid library, 200 µl of diluted cell mixture was spread with glass beads on 25 petri dishes (145
683 mm) containing mGAM with 25 µg/ml erythromycin and 200 µg/ml gentamicin. For the liquid
684 library, 3.5 ml of diluted cell mixture was added to 100 ml of mGAM with 25 µg/ml erythromycin
685 and 200 µg/ml gentamicin. Solid and liquid libraries were incubated anaerobically at 37°C for
686 32 hours. One ml of the outgrown liquid library was serially diluted 10-fold and plated on
687 selective mGAM to determine the output transconjugant CFUs. For the solid library, all
688 colonies were scraped and mixed in 131.5 ml mGAM containing 25 µg/ml erythromycin and
689 12% glycerol. The 100 ml liquid library was mixed with 31.5 ml of 50% glycerol. Multiple single-
690 use 1 ml cryostocks were created and stored at -80°C. The mutant library of *P. merdae* ATCC
691 43184 was constructed as above with the following modifications. *E. coli* donor library was
692 thawed from a second-generation glycerol stock, after previous amplification of the original *E.*
693 *coli* donor library. The time of aerobic conjugation was 14 hours. For the solid library, the
694 conjugation mix was plated with disposable L shape spreaders in 20 x 145 mm plates and 4
695 x 500 mm plates, and colonies were obtained after 48 h in anaerobic culturing at 37°C. Plates
696 were scraped and added to mGAM broth before mixing with glycerol to 24% w/v and stored
697 as 1 ml single-use pooled *P. merdae* library aliquots.
698
699 **Library preparation for TnSeq**
700 For *B. uniformis* and *P. vulgatus* mutant libraries, genomic DNA was extracted from one 1 ml
701 cryovial using the ZymoBiomics DNA miniprep kit (Zymo Research; D4300), while *P. merdae*
702 DNA was extracted with the DNAeasy PowerBiofilm kit (Qiagen, 24000-50). A two-step PCR
703 was performed to amplify transposon-genome junctions and prepare library DNA for Illumina
704 sequencing. Five identical PCR-1 reaction mixtures were prepared per library containing: 10
705 µl KAPA HiFi HotStart Readymix (Roche; KK2601), 160 nM PCR-1 forward primer, 160 nM

706 PCR-1 reverse primer 1, 160 nM PCR-1 reverse primer 2, 200 ng of library DNA and water up
707 to 20 µl total (see Supplementary table 6 for primer sequences). PCR-1 program was: 98°C
708 for 5 min, 6 cycles with [98°C for 30 sec, 42°C for 30 sec and -1°C per cycle, 72°C for 90 sec],
709 25 cycles with [98°C for 30 sec, 45°C for 30 sec, 72°C for 90 sec], 72°C for 10 min. PCR-1
710 reactions were pooled, purified using the GeneJET DNA Cleanup kit (TFS; K0831) and
711 quantified using a Qubit fluorometer (TFS). Four identical PCR-2 reaction mixtures were
712 prepared per library containing: 25 µl KAPA HiFi HotStart Readymix, 25 nM PCR-2 forward
713 primer 1, 25 nM PCR-2 forward primer 2, 25 nM PCR-2 forward primer 3, 25 nM PCR-2
714 forward primer 4, 100 nM PCR-2 reverse primer, 40 ng DNA from PCR-1, water up to 50 µl.
715 PCR-2 program was: 98°C for 5 min, 30 cycles with [98°C for 30 sec, 52°C for 30 sec, 72°C
716 for 90 sec], 72°C for 10 min. PCR-2 reactions were pooled, purified using the GeneJET DNA
717 Cleanup kit (TFS; K0831) and run on a 1.5% agarose gel. The expected DNA smear was cut
718 between 300 and 900 bps and extracted from gel using the GeneJET Gel Extraction and DNA
719 Cleanup Micro Kit. Library quality was assessed with a Bioanalyzer on a high sensitivity DNA
720 chip (Agilent) or Tapestation D5000 HS (Agilent). Libraries were sequenced on an Illumina
721 NextSeq 500 system with a Mid output flow cell for 150 basepair single-end reads and 10%
722 PhiX spike-in. Yield was at least 20 million reads per library.
723
724 **Insertion mapping using TnSeeker and barcode filtering**
725 Transposon insertions were mapped onto the genome using TnSeeker version 1.0.6.5
726 (https://github.com/afombravo/tnseeker) and Bowtie2 version 2.4.4[102] and a genome feature
727 file (GFF) which was obtained by running the mettannotator annotation pipeline[51]. The
728 following TnSeeker input parameters were used: --tn
729 TACGAAGACCGGGGACTTATCATCCAACCTG (Himar-1 inverted repeat), --m 6, --b, --b1
730 ATGTCCACGAGGTGTAACTG (*B. uniformis* and *P. merdae*) or
731 ATGTCCACGAGGTGTATGCA (*P. vulgatus*), --b2 CAGAATTGGGAGTCTACGAA, --b1m 3,
732 --b2m 3, --b1p 1, --b2p 1, --ph 10, --mq 1, --ne. The TnSeeker output file
733 "annotated_barcodes.csv" was used to determine the number of unique barcodes per gene
734 based on rules similar to those described in Price *et al.,*[14]. Briefly, good barcodes are defined
735 as either uniquely mapping to one genome position with 5 or more reads, or mapping to more
736 than one location with 10 or more reads of which 3/4 or more of the reads map to one primary
737 location and 1/8 or less of the reads map to any other location. To filter out likely erroneous
738 barcodes generated from sequencing errors, barcodes with a Hamming distance of 3 or less
739 compared to the barcode with the highest read count at a given position were removed.
740
741 **Analysis of gene essentiality**
742 An overview of the computational workflow and the required files and R scripts necessary for
743 essential gene analysis is shown in Supplementary figure 1. For the identification of essential
744 genes, we used the TRANSIT software package[54]. The necessary .prot_table and .wig file
745 inputs for TRANSIT were generated with custom R scripts. Only genes encoding proteins
746 between 10 and 5000 amino acids were included in the analysis (these thresholds are set
747 when making the .prot_table file). We used TRANSIT version 3.3.2 through the graphical user
748 interface. To determine essential genes with the HMM method, we used the following settings:
749 ignore N-terminus %: 5, ignore C-terminus %: 10, normalization: nonorm, replicates: sum, and
750 with correction for genome positional bias. The resulting output was run through the HMM
751 post-processing script (downloaded from https://github.com/mad-
752 lab/transit/tree/master/src/HMM_conf.py) to add confidence flags to the HMM calls[103]. The
753 HMM outputs one of four calls for each gene: essential (ES), growth defect (GD), not essential

754 (NE) or growth advantage (GA). To create a binary essentiality call, we combined GD genes
755 with ES genes if the GD gene had no reads. GD genes were combined with NE genes if they
756 had reads. GA genes were combined with NE genes. To determine essential genes with the
757 Gumbel-binomial method[104], we used the following settings: ignore N-terminus %: 5, ignore
758 C-terminus %: 10, samples: 20000, burn-in: 1000, trim: 1, minimum: 1, replicate: sum.
759 Essentiality calls from the HMM and Gumbel-binomial output were consolidated per library
760 and these calls were further consolidated between the liquid and solid libraries using a custom
761 R script according to the algorithm shown in Extended Data. Fig. 3A.
762
763 **Analyses of essential gene conservation and functional enrichment**
764 To determine the conservation of gene essentiality across species, we grouped genes into
765 families by mapping the protein-coding genes of the three species to the EggNOG 5.0
766 database[56] using EggNOG-mapper[105]. Gene families were defined based on COG
767 classification at the Bacteroidia (class) taxonomic level. PFAM annotations from EggNOG-
768 mapper were used as an alternative grouping method. Genes annotated as essential in either
769 liquid or solid media were classified as essential, while families containing genes with an
770 "unclear" essentiality call were excluded (n = 71). Families lacking gene members from one or
771 two species (n = 63) were analyzed by protein BLASTP (version 2.15.0+). Protein sequences
772 of the genes in these families were queried against the complete proteomes of *P. merdae*, *P.*
773 *vulgatus*, and *B. uniformis*. For each query, the top five subject hits were selected based on
774 the highest bitscore (ties resolved by the lowest E-value). These subject hits were
775 subsequently used as queries in reverse BLASTP searches against the proteome of the
776 original query species. The best hit was defined as the alignment with the highest bitscore,
777 with ties resolved by the lowest E-value. Reciprocal best hits (RBHs) were defined as gene
778 pairs that were each other's best forward and reverse hits. Hits were required to meet the
779 following thresholds: query coverage >= 80%, subject coverage >= 80%, bitscore >= 80, and
780 E-value <= 1e-20. RBHs involving three species were consolidated such that if two genes
781 shared the same COG assignment, the third was reassigned to that family. In cases of three
782 different family assignments or two-species RBHs, the family of the query species was
783 adopted. This procedure resulted in the reassignment of 14 genes, reducing the total number
784 of essential gene families from 452 (EggNOG only) to 438 after RBH-based correction. The
785 COG category enrichment analysis was performed using the categories listed per gene family
786 (eggNOG COG at Bacteroidia level) from the eggNOG-mapper output with a custom R script.
787 The COG categories were retrieved from NCBI. Enrichment was assessed using a one-sided
788 Fisher's exact test. *p*-values were adjusted for multiple testing using the Benjamini–Hochberg
789 false discovery rate (FDR) method.
790
791 **Analysis of essential protein domains**
792 To evaluate the essentiality of protein domains encoded within genes, we annotated the
793 genome at the domain level using InterProScan outputs derived from the mettannotator
794 pipeline and a custom R script. Briefly: for each domain prediction tool in the InterProScan
795 output (e.g., PFAM, NCBIfam), the longest (in nucleotides) entries labeled as "Domain" or
796 "Family" were retained. Domains were prioritized over families, and redundant annotations
797 (e.g., domains embedded in families or vice versa) were removed. Predictions with >50%
798 overlap were consolidated, retaining only the longest prediction (e.g., PFAM prediction
799 retained over a shorter NCBIfam prediction). Inter-domain regions were labeled sequentially
800 (e.g., region_1, region_2), starting from the 5' end of each gene. A new .prot_table file was
801 generated using the domain-annotated genome file, retaining only domains and regions ≥10

802 amino acids. The .prot_table was used together with library-specific .wig files of insertion
803 counts at TA sites for domain-essentiality assessment using TRANSIT's HMM method. For
804 the domain-essentiality analysis, unlike in the gene-essentiality analysis, insertions in the N-
805 or C-terminus of proteins were not ignored. The HMM output classified TA sites within domains
806 and regions as "essential" (ES), "growth defect" (GD), "non-essential" (NE), or "growth
807 advantage" (GA) and to create a binary call, GD sites were converted to ES sites if they had
808 no read counts and were converted to NE sites if they had read counts. GA sites were
809 converted to NE sites. To summarize the percentage of essential TA sites in domains and
810 regions per gene, those genes found to be essential in either solid or liquid media were
811 counted as essential genes. To call hits of essential genes containing non-essential protein
812 domains, or vice versa, we selected genes with at least two domains, each represented by at
813 least 10 TA sites and without a low-confidence HMM flag. Among these, one domain had to
814 have the highest HMM probability of being essential, while another had to have the highest
815 probability other than being essential. The TRANSIT's HMM essentiality output per domain
816 and selection of hits is included in Supplementary table 3. AlphaFold monomer-predicted
817 structures of proteins of interest were retrieved from UniProt using their accession codes.
818 To find structural homologues of *E. coli* FabZ and LpxC, we first generated structural
819 predictions of all proteins of the three species using ProstT5[106] as implemented within
820 the Phold package and using its default settings (version 0.1.3)[107]. These predicted structures
821 were searched against the PDB (Aug-2024) using foldseek[73] (version 9.427df8a), using
822 default settings for the easy-search mode. Proteins with predicted structural similarities to
823 FabZ (6n3p[72]) and LpxC (4mdt[71]) and E-values < 0.05 were retained. Alphafold models of the
824 hits were retrieved from UniProt using each protein's UniProt accession and were run in the
825 foldseek webserver (Aug-2025) for visual inspection and final model scores (RMSD, E-value,
826 TM-score).
827
828 **Analysis of insertion directionality bias**
829 Directionality bias was assessed using a custom R script. For each gene, the directionality
830 ratio was calculated as the number of insertions in the gene's sense strand divided by the total
831 insertions in both the sense and antisense strands. Ratios were median-normalized across all
832 libraries. Directionality bias significance was determined using a binomial test with Benjamini-
833 Hochberg correction. Genes with an adjusted *p*-value < 0.01 and a directionality ratio < 0.2 or
834 > 0.8 were classified as significantly biased. Putative toxin and antitoxin genes were identified
835 in the three species using two approaches: Searching for "toxin" or "antitoxin" in the gene
836 description fields of the .gff output files generated by mettannotator and by using
837 TAfinder2.0[108] via the web interface with the following parameters: BLAST E-value: 0.01;
838 HMMER E-value: 0.01; Maximum sequence length: 500 amino acids; Maximum distance: 150
839 nucleotides; Maximum overlap: 50 nucleotides. The input file was a .gbk file generated by
840 mettannotator. Supplementary table 4 includes directionality bias ratios for all genes across
841 libraries, significantly biased genes and their immediate neighbors, canonical toxin-antitoxin
842 genes found using text mining and TAfinder2.0, and genes with similar directionality biases to
843 toxin-antitoxin pairs.
844
845 **Supplementary material**
846 Supplementary table 1: Essentiality calls for all annotated features in the liquid and solid
847 mutant libraries of *P. merdae*, *B. uniformis* and *P. vulgatus* (tab1) and conservation status of
848 essential genes (tab2)
849 Supplementary table 2: Reciprocal best hit BLAST results for finding orthologs

Supplementary table 3: Essentiality calls for each domain and region within genes in the liquid and solid mutant libraries of *P. merdae*, *B. uniformis* and *P. vulgatus* (tab1) and selected genes with domain essentiality (tab2)
Supplementary table 4: Insertion directionality ratios of all coding features in the liquid and solid mutant libraries of *P. merdae*, *B. uniformis* and *P. vulgatus* (tab1), genes with directionality bias and their neighbors (tab2), gene-pairs resembling toxin-antitoxin systems (tab3) and canonical toxin-antitoxins in *P. merdae*, *B. uniformis* and *P. vulgatus* (tab4)
Supplementary table 5: Strains used in this study
Supplementary table 6: DNA oligos used in this study
Supplementary figure 1: Inputs, outputs, scripts and softwares used to perform functional genomics analyses
Supplementary file 1: Annotated plasmid sequence of pCV006 (ermG version)

Data availability

Sequencing data of the *P. merdae* mutant libraries has been deposited in the European Nucleotide Archive (ENA) at EMBL-EBI under accession number PRJEB77289. Sequencing data of *B. uniformis* and *P. vulgatus* libraries has been deposited in the ENA under accession number PRJEB98479 and will be available after 01-July-2026. Whole genome sequences of *P. merdae* ATCC43184, *B. uniformis* ATCC8492 and *P. vulgatus* ATCC8482 and strains isolated from fecal samples in this work are deposited in the ENA under study number ERP180871 and will be available after 01-July-2026.

Code availability

TnSeeker software, used for processing of TnSeq reads, is available at https://github.com/afombravo/tnseeker. Custom Unix and R scripts to perform functional genomics analyses of a single Mariner based TnSeq library are available at https://git.embl.org/grp-typas/transposon_toolkit. See Supplementary figure 1 for a flowchart of files, scripts and softwares used for the analyses.

Acknowledgements

We thank Vitalina Chamberlain-Evans (MRC Toxicology Unit, University of Cambridge) for helpful conversation and guidance on DNA library QC. We thank all Typas group members for helpful discussions and in particular, Tara Bartolec for running and providing Foldseek output and Martin Garrido Rodriguez-Cordoba for assistance with Alphafold modelling. We thank Justin Sonnenburg for providing the pWW3864 plasmid. We thank the EMBL genomics core facility, and in particular Vladimir Benes, Mireia Osuna Lopez and Hilal Ozgur for their help and support with whole genome and TnSeq sequencing library preparation.

Author contributions

Conceptualization: C.V., I.R., M.Z, K.R.P., A.T. Funding acquisition: C.V., M.Z, K.R.P., A.T. Experiments: C.V., I.R., K.M., J.B. Data analysis: C.V., I.R., N.K., A.B., L.K., V.V. Writing manuscript: C.V., I.R., A.T. with edits from all authors. Visualization: C.V., I.R. Supervision: G.Z., M.Z., K.R.P., A.T.

Funding

This work was funded by ERC grant uCARE ID 819454 (to A.T.), the Liliane Bettencourt Prize for Life Sciences (to A.T.), ERC grant GutTransForm ID 101078353 (to M.Z.), and a grant from the EMBL | Stanford Data Creation Fund provided by the Life Science Alliance (to A.T.). EMBL

Core funding and especially dedicated funding from the Microbial Ecosystems Transversal Theme contributed to this project. C.V. was supported by a fellowship from the EMBL Interdisciplinary Postdoc (EIPOD4) program under the Marie Skłodowska-Curie Actions COFUND (grant 847543) and by an Add-On Fellowship for Interdisciplinary Science from the Joachim Herz Foundation for parts of the project. This project has received funding from the European Research Council (ERC) under the European Union's Horizon 2020 research and innovation programme (grant ID 866028) (KRP and IR) and from the UK Medical Research Council (project ID MC_UU_00025/11) (KRP).

Conflict of interest

The authors declare no conflict of interest.

References

1. Qin, J. *et al.* A human gut microbial gene catalogue established by metagenomic sequencing. *Nature* **464**, 59–65 (2010).
2. The Human Microbiome Jumpstart Reference Strains Consortium *et al.* A catalog of reference genomes from the human microbiome. *Science* **328**, 994–999 (2010).
3. Sereika, M. *et al.* Genome-resolved long-read sequencing expands known microbial diversity across terrestrial habitats. *Nat. Microbiol.* **10**, 2018–2030 (2025).
4. Almeida, A. *et al.* A unified catalog of 204,938 reference genomes from the human gut microbiome. *Nat. Biotechnol.* **39**, 105–114 (2021).
5. Coelho, L. P. *et al.* Towards the biogeography of prokaryotic genes. *Nature* **601**, 252–256 (2022).
6. Schmidt, T. S. B. *et al.* SPIRE: a Searchable, Planetary-scale mIcrobiome REsource. *Nucleic Acids Res.* **52**, D777–D783 (2024).
7. Moore, L. R. *et al.* Revisiting the y-ome of *Escherichia coli*. *Nucleic Acids Res.* **52**, 12201–12207 (2024).
8. Wicke, D., Meißner, J., Warneke, R., Elfmann, C. & Stülke, J. Understudied proteins and understudied functions in the model bacterium *Bacillus subtilis*—A major challenge in current research. *Mol. Microbiol.* **120**, 8–19 (2023).
9. Jana, B. *et al.* CRISPRi–TnSeq maps genome-wide interactions between essential and non-essential genes in bacteria. *Nat. Microbiol.* **9**, 2395–2409 (2024).
10. Koo, B.-M. *et al.* Comprehensive double-mutant analysis of the *Bacillus subtilis* envelope using double-CRISPRi. Preprint at *bioRxiv* https://doi.org/10.1101/2024.08.14.608006 (2024).
11. Brochado, A. R. & Typas, A. High-throughput approaches to understanding gene function and mapping network architecture in bacteria. *Curr. Opin. Microbiol.* **16**, 199–206 (2013).
12. Liu, H. & Deutschbauer, A. M. Rapidly moving new bacteria to model-organism status. *Curr. Opin. Biotechnol.* **51**, 116–122 (2018).
13. Nichols, R. J. *et al.* Phenotypic landscape of a bacterial cell. *Cell* **144**, 143–156 (2011).
14. Price, M. N. *et al.* Mutant phenotypes for thousands of bacterial genes of unknown function. *Nature* **557**, 503–509 (2018).
15. Mazurkiewicz, P., Tang, C. M., Boone, C. & Holden, D. W. Signature-tagged mutagenesis: barcoding mutants for genome-wide screens. *Nat. Rev. Genet.* **7**, 929–939 (2006).
16. Wetmore, K. M. *et al.* Rapid quantification of mutant fitness in diverse bacteria by sequencing randomly bar-coded transposons. *mBio* **6**, e00306-15 (2015).
17. Cain, A. K. *et al.* A decade of advances in transposon-insertion sequencing. *Nat. Rev. Genet.* **21**, 526–540 (2020).
18. Tripathi, S. *et al.* Randomly barcoded transposon mutant libraries for gut commensals I: Strategies for efficient library construction. *Cell Rep.* **43**, 113517 (2024).
19. Voogdt, C. G. P. *et al.* Randomly barcoded transposon mutant libraries for gut commensals II: Applying libraries for functional genetics. *Cell Rep.* **43**, 113519 (2024).
20. Cullen, T. W. *et al.* Antimicrobial peptide resistance mediates resilience of prominent gut commensals during inflammation. *Science* **347**, 170–175 (2015).
21. Liu, H. *et al.* Functional genetics of human gut commensal *Bacteroides thetaiotaomicron* reveals metabolic requirements for growth across environments. *Cell Rep.* **34**, (2021).
22. Shiver, A. L. *et al.* Genome-scale resources in the infant gut symbiont *Bifidobacterium breve* reveal genetic determinants of colonization and host-microbe interactions. *Cell* **188**, 2003-2021.e19 (2025).
23. Juhas, M., Eberl, L. & Church, G. M. Essential genes as antimicrobial targets and cornerstones of synthetic biology. *Trends Biotechnol.* **30**, 601–607 (2012).
24. Christen, B. *et al.* The essential genome of a bacterium. *Mol. Syst. Biol.* **7**, 528 (2011).
25. Goodall, E. C. A. *et al.* The essential genome of *Escherichia coli* K-12. *mBio* **9**, (2018).

26. Rancati, G., Moffat, J., Typas, A. & Pavelka, N. Emerging and evolving concepts in gene essentiality. *Nat. Rev. Genet.* **19**, 34–49 (2018).
27. Rousset, F. *et al.* The impact of genetic diversity on gene essentiality within the *Escherichia coli* species. *Nat. Microbiol.* **6**, 301–312 (2021).
28. Zhu, A., Sunagawa, S., Mende, D. R. & Bork, P. Inter-individual differences in the gene content of human gut bacterial species. *Genome Biol.* **16**, 82 (2015).
29. Madi, N., Chen, D., Wolff, R., Shapiro, B. J. & Garud, N. R. Community diversity is associated with intra-species genetic diversity and gene loss in the human gut microbiome. *eLife* **12**, e78530 (2023).
30. Dale, J. L. *et al.* Comprehensive functional analysis of the *Enterococcus faecalis* core genome using an ordered, sequence-defined collection of insertional mutations in strain OG1RF. *mSystems* **3**, e00062-18 (2018).
31. Davey, L. E. *et al.* A genetic system for *Akkermansia muciniphila* reveals a role for mucin foraging in gut colonization and host sterol biosynthesis gene expression. *Nat. Microbiol.* **8**, 1450–1467 (2023).
32. Dembek, M. *et al.* High-throughput analysis of gene essentiality and sporulation in *Clostridium difficile*. *mBio* **6**, e02383-14 (2015).
33. Ito, M. *et al.* Transposon mutagenesis of probiotic *Lactobacillus casei* identifies asnH, an asparagine synthetase gene involved in its immune-activating capacity. *PLoS One* **9**, e83876 (2014).
34. Fiebig, A. *et al.* Bile acid fitness determinants of a *Bacteroides fragilis* isolate from a human pouchitis patient. *mBio* **15**, e02830-23 (2023).
35. Goodman, A. L. *et al.* Identifying genetic determinants needed to establish a human gut symbiont in its habitat. *Cell Host Microbe* **6**, 279–289 (2009).
36. Huang, Y. Y. *et al.* Barcoded overexpression screens in gut Bacteroidales identify genes with roles in carbon utilization and stress resistance. *Nat. Commun.* **15**, 6618 (2024).
37. Veeranagouda, Y., Husain, F., Tenorio, E. L. & Wexler, H. M. Identification of genes required for the survival of *B. fragilis* using massive parallel sequencing of a saturated transposon mutant library. *BMC Genomics* **15**, 429 (2014).
38. Wu, M. *et al.* Genetic determinants of in vivo fitness and diet responsiveness in multiple human gut *Bacteroides*. *Science* **350**, (2015).
39. Wexler, A. G. & Goodman, A. L. An insider's perspective: *Bacteroides* as a window into the microbiome. *Nat. Microbiol.* **2**, 17026 (2017).
40. Wexler, H. M. *Bacteroides*: the Good, the Bad, and the Nitty-Gritty. *Clin. Microbiol. Rev.* **20**, 593–621 (2007).
41. Zafar, H. & Saier Jr, M. H. Gut *Bacteroides* species in health and disease. *Gut Microbes* **13**, 1848158 (2021).
42. Horvath, T. D. *et al. Bacteroides ovatus* colonization influences the abundance of intestinal short chain fatty acids and neurotransmitters. *iScience* **25**, 104158 (2022).
43. Whitaker, W. R., Shepherd, E. S. & Sonnenburg, J. L. Tunable expression tools enable single-cell strain distinction in the gut microbiome. *Cell* **169**, 538-546.e12 (2017).
44. Bayley, D. P., Rocha, E. R. & Smith, C. J. Analysis of *cepA* and other *Bacteroides fragilis* genes reveals a unique promoter structure. *FEMS Microbiol. Lett.* **193**, 149–154 (2000).
45. Engler, C., Gruetzner, R., Kandzia, R. & Marillonnet, S. Golden Gate shuffling: A one-pot DNA shuffling method based on type IIs restriction enzymes. *PLoS ONE* **4**, e5553 (2009).
46. Liu, H. *et al.* Magic pools: Parallel assessment of transposon delivery vectors in bacteria. *mSystems* **3**, e00143-17 (2018).
47. García-Bayona, L. & Comstock, L. E. Streamlined genetic manipulation of diverse *Bacteroides* and *Parabacteroides* isolates from the human gut microbiota. *mBio* **10**, 10.1128/mbio.01762-19 (2019).
48. Ronda, C., Chen, S. P., Cabral, V., Yaung, S. J. & Wang, H. H. Metagenomic engineering of the mammalian gut microbiome in situ. *Nat. Methods* **16**, 167–170 (2019).
49. Bobonis, J., Yang, A. L. J., Voogdt, C. G. P. & Typas, A. TAC–TIC, a high-throughput genetics method to identify triggers or blockers of bacterial toxin–antitoxin systems. *Nat. Protoc.* **19**, 2231–2249 (2024).
50. Ferrières, L. *et al.* Silent mischief: Bacteriophage Mu insertions contaminate products of *Escherichia coli* random mutagenesis performed using suicidal transposon delivery plasmids mobilized by broad-host-range RP4 conjugative machinery. *J. Bacteriol.* **192**, 6418–6427 (2010).
51. Gurbich, T. A., Beracochea, M., De Silva, N. H. & Finn, R. D. mettannotator: a comprehensive and scalable Nextflow annotation pipeline for prokaryotic assemblies. *Bioinformatics* **41**, btaf037 (2025).
52. van Opijnen, T., Bodi, K. L. & Camilli, A. Tn-seq: high-throughput parallel sequencing for fitness and genetic interaction studies in microorganisms. *Nat. Methods* **6**, 767–772 (2009).
53. Anzai, I. A., Shaket, L., Adesina, O., Baym, M. & Barstow, B. Rapid curation of gene disruption collections using Knockout Sudoku. *Nat. Protocols* **12**, 2110–2137 (2017).
54. DeJesus, M. A., Ambadipudi, C., Baker, R., Sassetti, C. & Ioerger, T. R. TRANSIT - A software tool for Himar1 TnSeq analysis. *PLoS Comput. Biol.* **11**, e1004401 (2015).
55. A. Ghomi, F. *et al.* High-throughput transposon mutagenesis in the family Enterobacteriaceae reveals core essential genes and rapid turnover of essentiality. *mBio* **0**, e01798-24 (2024).
56. Huerta-Cepas, J. *et al.* eggNOG 5.0: a hierarchical, functionally and phylogenetically annotated orthology resource based on 5090 organisms and 2502 viruses. *Nucleic Acids Res.* **47**, D309–D314 (2019).
57. Rodionov, D. A. *et al.* Transcriptional regulation of NAD metabolism in bacteria: NrtR family of Nudix-related regulators. *Nucleic Acids Res.* **36**, 2047–2059 (2008).

58. Seif, Y. *et al.* Metabolic and genetic basis for auxotrophies in Gram-negative species. *Proc. Natl. Acad. Sci. U S A* **117**, 6264–6273 (2020).
59. Osterman, A. Biogenesis and homeostasis of nicotinamide adenine dinucleotide cofactor. *EcoSal Plus* **3**, 10.1128/ecosalplus.3.6.3.10 (2009).
60. Hannay, K., Marcotte, E. M. & Vogel, C. Buffering by gene duplicates: an analysis of molecular correlates and evolutionary conservation. *BMC Genomics* **9**, 609 (2008).
61. Jones, P. *et al.* InterProScan 5: genome-scale protein function classification. *Bioinformatics* **30**, 1236–1240 (2014).
62. Kornberg A, B. T. A. A. Kornberg, T.A. Baker DNA Replication (2nd Edition), Freeman, San Francisco, CA (1992), Pp. 113-164. (Freeman, San Francisco, CA, 1992).
63. Jumper, J. *et al.* Highly accurate protein structure prediction with AlphaFold. *Nature* **596**, 583–589 (2021).
64. Wu, H. *et al.* Research progress of LpxC inhibitor on Gram-negative bacteria. *Eur. J. Med. Chem.* **289**, 117440 (2025).
65. Carfrae, L. A. *et al.* Inhibiting fatty acid synthesis overcomes colistin resistance. *Nat. Microbiol.* **8**, 1026–1038 (2023).
66. Bibens, L., Becker, J.-P., Dassonville-Klimpt, A. & Sonnet, P. A Review of fatty acid biosynthesis enzyme inhibitors as promising antimicrobial drugs. *Pharmaceuticals* **16**, 425 (2023).
67. Dewachter, L. *et al.* Deep mutational scanning of essential bacterial proteins can guide antibiotic development. *Nat. Commun.* **14**, 241 (2023).
68. Zeng, D. *et al.* Mutants resistant to LpxC inhibitors by rebalancing cellular homeostasis. *J. Biol. Chem.* **288**, 5475–5486 (2013).
69. Mostafavi, M. *et al.* Interplay of *Klebsiella pneumoniae fabZ* and *lpxC* mutations leads to LpxC inhibitor-dependent growth resulting from loss of membrane homeostasis. *mSphere* **3**, 10.1128/msphere.00508-18 (2018).
70. Möller, A.-M. *et al.* LapB (YciM) orchestrates protein–protein interactions at the interface of lipopolysaccharide and phospholipid biosynthesis. *Mol. Microbiol.* **119**, 29–43 (2023).
71. Clayton, G. M. *et al.* Structure of the bacterial deacetylase LpxC bound to the nucleotide reaction product reveals mechanisms of oxyanion stabilization and proton transfer. *J. Biol. Chem.* **288**, 34073–34080 (2013).
72. Dodge, G. J. *et al.* Structural and dynamical rationale for fatty acid unsaturation in *Escherichia coli*. *Proc. Natl. Acad. Sci. U S A* **116**, 6775–6783 (2019).
73. van Kempen, M. *et al.* Fast and accurate protein structure search with Foldseek. *Nat. Biotechnol.* **42**, 243–246 (2024).
74. Keiler, K. C. Biology of trans-Translation. *Annu. Rev. Microbiol.* **62**, 133–151 (2008).
75. Chadani, Y. *et al.* Ribosome rescue by *Escherichia coli* ArfA (YhdL) in the absence of trans-translation system. *Mol. Microbiol.* **78**, 796–808 (2010).
76. Chadani, Y., Ono, K., Kutsukake, K. & Abo, T. *Escherichia coli* YaeJ protein mediates a novel ribosome-rescue pathway distinct from SsrA- and ArfA-mediated pathways. *Mol. Microbiol.* **80**, 772–785 (2011).
77. Handa, Y., Inaho, N. & Nameki, N. YaeJ is a novel ribosome-associated protein in *Escherichia coli* that can hydrolyze peptidyl–tRNA on stalled ribosomes. *Nucleic Acids Res.* **39**, 1739–1748 (2011).
78. Hampton, H. G. *et al.* Functional genomics reveals the toxin–antitoxin repertoire and AbiE activity in *Serratia*. *Microb. Genom.* **6**, e000458 (2020).
79. Hutchison, C. A. *et al.* Polar effects of transposon insertion into a minimal bacterial genome. *J. Bacteriol.* **201**, 10.1128/jb.00185-19 (2019).
80. Fineran, P. C. *et al.* The phage abortive infection system, ToxIN, functions as a protein–RNA toxin–antitoxin pair. *Proc. Natl. Acad. Sci.* **106**, 894–899 (2009).
81. Parke, D. & Ornston, L. N. Toxicity caused by hydroxycinnamoyl-coenzyme A thioester accumulation in mutants of *Acinetobacter* sp. strain ADP1. *Appl. Environ. Microbiol.* **70**, 2974–2983 (2004).
82. Sabag-Daigle, A. *et al.* A metabolic intermediate of the fructose-asparagine utilization pathway inhibits growth of a *Salmonella* fraB mutant. *Sci. Rep.* **6**, 28117 (2016).
83. Campbell, D. E. *et al.* Infection with *Bacteroides* phage BV01 alters the host transcriptome and bile acid metabolism in a common human gut microbe. *Cell Rep.* **32**, 108142 (2020).
84. Peters, J. M. *et al.* A comprehensive, CRISPR-based functional analysis of essential genes in bacteria. *Cell* **165**, 1493–1506 (2016).
85. Bernstein, D. B., Akkas, B., Price, M. N. & Arkin, A. P. Evaluating *E. coli* genome-scale metabolic model accuracy with high-throughput mutant fitness data. *Mol. Syst. Biol.* **19**, e11566 (2023).
86. Mobegi, F. M. *et al.* From microbial gene essentiality to novel antimicrobial drug targets. *BMC Genomics* **15**, 958 (2014).
87. Amrofell, M. B. *et al.* Engineering *E. coli* strains using antibiotic-resistance-gene-free plasmids. *Cell Rep. Methods* **3**, (2023).
88. Lopez, G. & Anderson, J. C. Synthetic auxotrophs with ligand-dependent essential genes for a BL21(DE3) biosafety strain. *ACS Synth. Biol.* **4**, 1279–1286 (2015).
89. Koo, B.-M. *et al.* Construction and analysis of two genome-scale deletion libraries for *Bacillus subtilis*. *Cell Syst.* **4**, 291-305.e7 (2017).
90. Lau, A. M. *et al.* Exploring structural diversity across the protein universe with The Encyclopedia of Domains. *Science* **386**, eadq4946 (2024).

91. DeJesus, M. A. *et al.* Comprehensive essentiality analysis of the *Mycobacterium tuberculosis* genome via saturating transposon mutagenesis. *mBio* **8**, 10.1128/mbio.02133-16 (2017).
92. Lagator, M. *et al.* Predicting bacterial promoter function and evolution from random sequences. *eLife* **11**, e64543 (2022).
93. Taheri Ghahfarokhi, S. M. A. & Peña-Castillo, L. BacTermFinder: a comprehensive and general bacterial terminator finder using a CNN ensemble. *NAR Genom. Bioinform.* **7**, lqaf016 (2025).
94. Johnson, C. M. & Grossman, A. D. Identification of host genes that affect acquisition of an integrative and conjugative element in *Bacillus subtilis*. *Mol. Microbiol.* **93**, 1284–1301 (2014).
95. Pérez-Mendoza, D. & de la Cruz, F. *Escherichia coli* genes affecting recipient ability in plasmid conjugation: Are there any? *BMC Genomics* **10**, 71 (2009).
96. Yang, X., Xu, M. & Yang, S.-T. Restriction modification system analysis and development of in vivo methylation for the transformation of *Clostridium cellulovorans*. *Appl. Microbiol. Biotechnol.* **100**, 2289–2299 (2016).
97. Brophy, J. A. N. *et al.* Engineered integrative and conjugative elements for efficient and inducible DNA transfer to undomesticated bacteria. *Nat. Microbiol.* **3**, 1043–1053 (2018).
98. Mimee, M., Tucker, A. C., Voigt, C. A. & Lu, T. K. Programming a human commensal bacterium, *Bacteroides thetaiotaomicron*, to sense and respond to stimuli in the murine gut microbiota. *Cell Syst.* **1**, 62–71 (2015).
99. Prezza, G., Liao, C., Reichardt, S., Beisel, C. L. & Westermann, A. J. CRISPR-based screening of small RNA modulators of bile susceptibility in *Bacteroides thetaiotaomicron*. *Proc. Natl. Acad. Sci. U S A***121**, e2311323121 (2024).
100. Kolmogorov, M., Yuan, J., Lin, Y. & Pevzner, P. A. Assembly of long, error-prone reads using repeat graphs. *Nat. Biotechnol.* **37**, 540–546 (2019).
101. Chaumeil, P.-A., Mussig, A. J., Hugenholtz, P. & Parks, D. H. GTDB-Tk: a toolkit to classify genomes with the Genome Taxonomy Database. *Bioinformatics* **36**, 1925–1927 (2020).
102. Langmead, B. & Salzberg, S. L. Fast gapped-read alignment with Bowtie 2. *Nat. Methods* **9**, 357–359 (2012).
103. DeJesus, M. A. & Ioerger, T. R. A Hidden Markov Model for identifying essential and growth-defect regions in bacterial genomes from transposon insertion sequencing data. *BMC Bioinformatics* **14**, 303 (2013).
104. DeJesus, M. A. *et al.* Bayesian analysis of gene essentiality based on sequencing of transposon insertion libraries. *Bioinformatics* **29**, 695–703 (2013).
105. Cantalapiedra, C. P., Hernández-Plaza, A., Letunic, I., Bork, P. & Huerta-Cepas, J. eggNOG-mapper v2: functional annotation, orthology assignments, and domain prediction at the metagenomic scale. *Mol. Biol. Evol.* **38**, 5825–5829 (2021).
106. Heinzinger, M. *et al.* Bilingual language model for protein sequence and structure. *NAR Genom. Bioinform.* **6**, lqae150 (2024).
107. Bouras, G. *et al.* Protein Structure Informed Bacteriophage Genome Annotation with Phold. Preprint at *bioRxiv* https://doi.org/10.1101/2025.08.05.668817 (2025).
108. Xie, Y. *et al.* TADB 2.0: an updated database of bacterial type II toxin–antitoxin loci. *Nucleic Acids Res.* **46**, D749–D753 (2018).
109. Ondov, B. D. *et al.* Mash: fast genome and metagenome distance estimation using MinHash. *Genome Biol.* **17**, 132 (2016).
110. Szklarczyk, D. *et al.* The STRING database in 2021: customizable protein–protein networks, and functional characterization of user-uploaded gene/measurement sets. *Nucleic Acids Res.* **49**, D605–D612 (2021).
111. Abramson, J. *et al.* Accurate structure prediction of biomolecular interactions with AlphaFold 3. *Nature* **630**, 493–500 (2024).

1138 **Figures with legends**
Figure 1

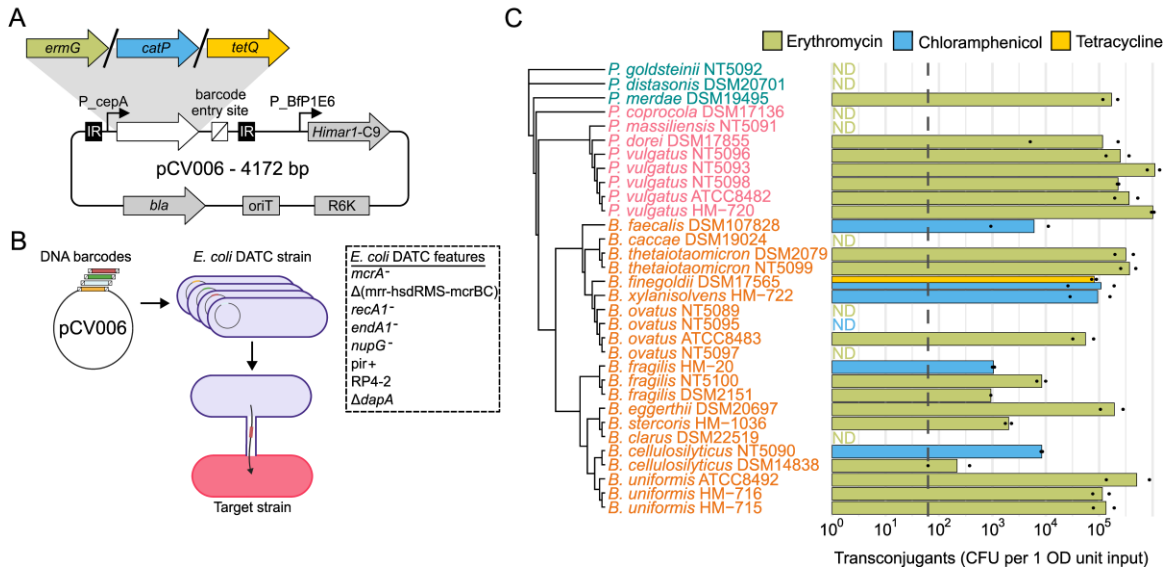

1139
1140 **Fig. 1: Optimized barcoded transposon mutagenesis in Bacteroidales. A)** A broad-host-
1141 range transposon vector series for Bacteroidales, carrying different selection markers and a
1142 BsmBI based cloning site (Golden Gate) for barcoding. The barcoded plasmid pools are also
1143 available. Expression of the transposase and selection markers are placed under conserved
1144 and constitutive Bacteroidales promoters. IR: inverted repeat, *bla*: beta-lactamase, *oriT*: origin
1145 of transfer, R6K: origin of replication, *himar1*-C9: transposase (mariner), *ermG*: rRNA adenine
1146 N-6-methyltransferase (erythromycin resistance), *catP*: chloramphenicol acetyltransferase,
1147 *tetQ*: tetracycline resistance protein. **B)** A universal donor strain for efficient broad-host range
1148 conjugation. The *E. coli* strain DATC can be used both for plasmid barcoding/cloning and
1149 conjugation. The schematic highlights some of its genomic features that facilitate both
1150 processes. **C)** The new universal donor strain and broad-host range vector series allow for
1151 high conjugation efficiency across three Bacteroidales genera. Conjugation efficiency of 32
1152 recipient strains of *Parabacteroides* (green), *Phocaeicola* (pink) and *Bacteroides* (orange), as
1153 the number (Colony Forming Units) of transconjugants per 1 OD unit of input cells (which is 1
1154 ml of saturated culture of OD = 1). ND: no transconjugants detected. Dashed line denotes the
1155 limit of detection. Bars indicate the mean CFU count of two biological replicates (replicates
1156 shown as black dots) on mGAM agar plates containing appropriate antibiotics. Strains are
1157 grouped by phylogeny according to a neighbor-joining tree built on whole genome average
1158 nucleotide identity approximated with Mash version 2.3[109].
1159

Figure 2

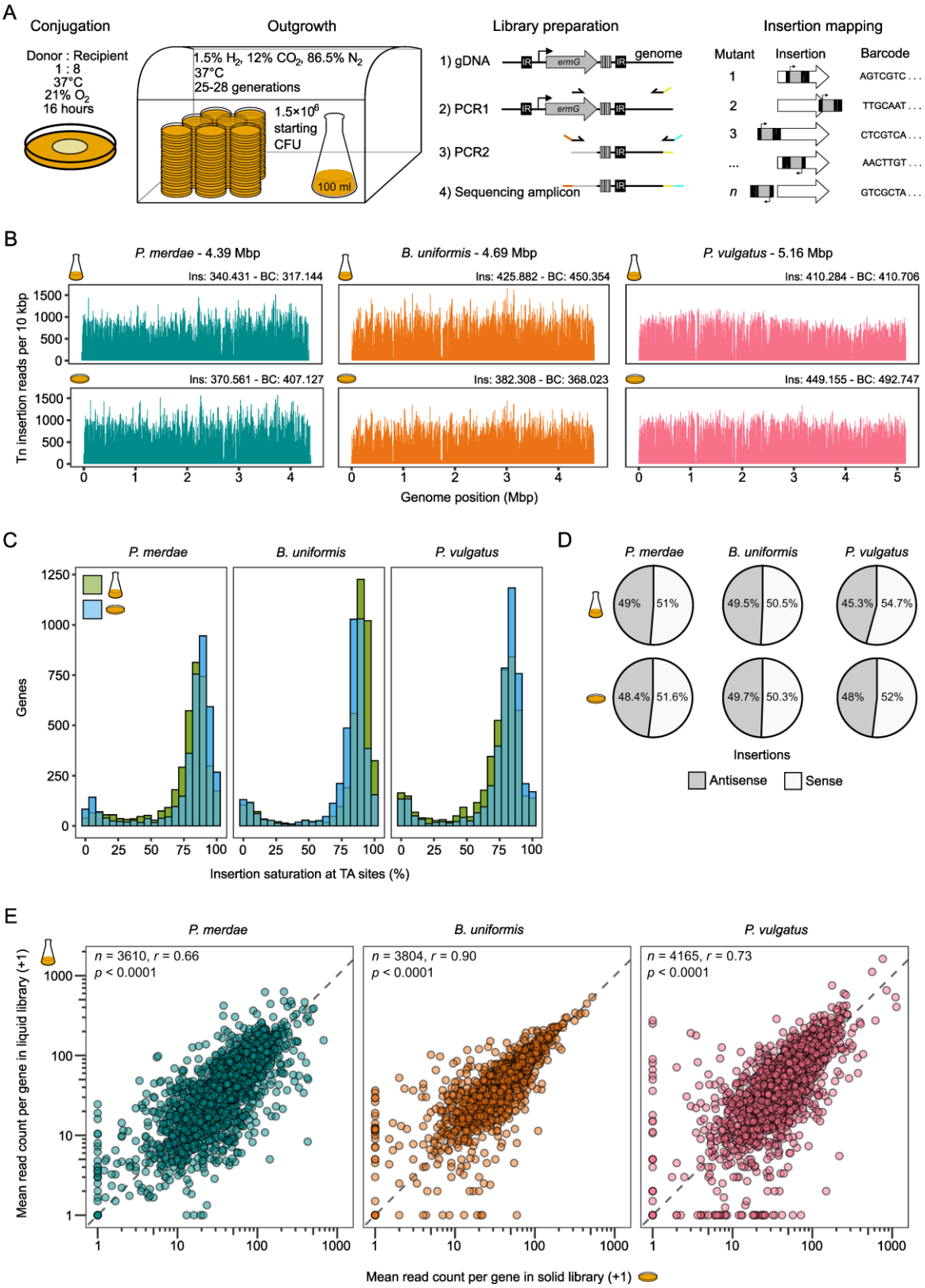

Fig. 2: Saturated barcoded transposon libraries in three Bacteroidales genera. A) Schematic of a simplified protocol to create transposon insertion libraries in Bacteroidales species. Following overnight conjugation on mGAM plates in aerobic conditions, ~1.5 million transconjugants are inoculated in liquid media (simplified method that improves handling) or

1165 plated on more than 25 large petri dishes (solid/conventional method). After 25–28
1166 generations of outgrowth, the liquid culture or colonies scraped from all plates are used for
1167 cryostocking and sequencing library preparation, which involves DNA extraction followed by
1168 two sequential PCRs to generate amplicons ready for sequencing. Insertion and barcode
1169 mapping are done using TnSeeker (Methods). **B)** Dense and unbiased transposon insertions
1170 into the genome of *P. merdae*, *B. uniformis* and *P. vulgatus* type strains. Transposon insertion
1171 coverage across the genome is shown as the sum of insertion reads per 10 kbp. Genome
1172 size, number of unique insertion positions (Ins) and unique barcodes (BC) are indicated above
1173 each plot. **C)** Most non-essential genes are highly saturated with insertions in all three species,
1174 independent of whether the conventional solid or simplified liquid protocol was used. Genes
1175 are binned based on the insertion saturation level of TA dinucleotide sites which is the number
1176 of TA sites with insertions as a percentage of all TA sites within a gene. **D)** Solid- and liquid-
1177 based libraries show no directionality bias of insertions in the sense (coding) or antisense
1178 strand of the targeted gene. **E)** Mutant abundance is similar in solid- and liquid-generated
1179 libraries. Shown is the mean read count of all mutants per gene. One count was added to the
1180 reads to enable visualization on a log scale. n = number of genes analyzed, r = Pearson
1181 correlation coefficient, p = p-value (two-sided).
1182

Figure 3

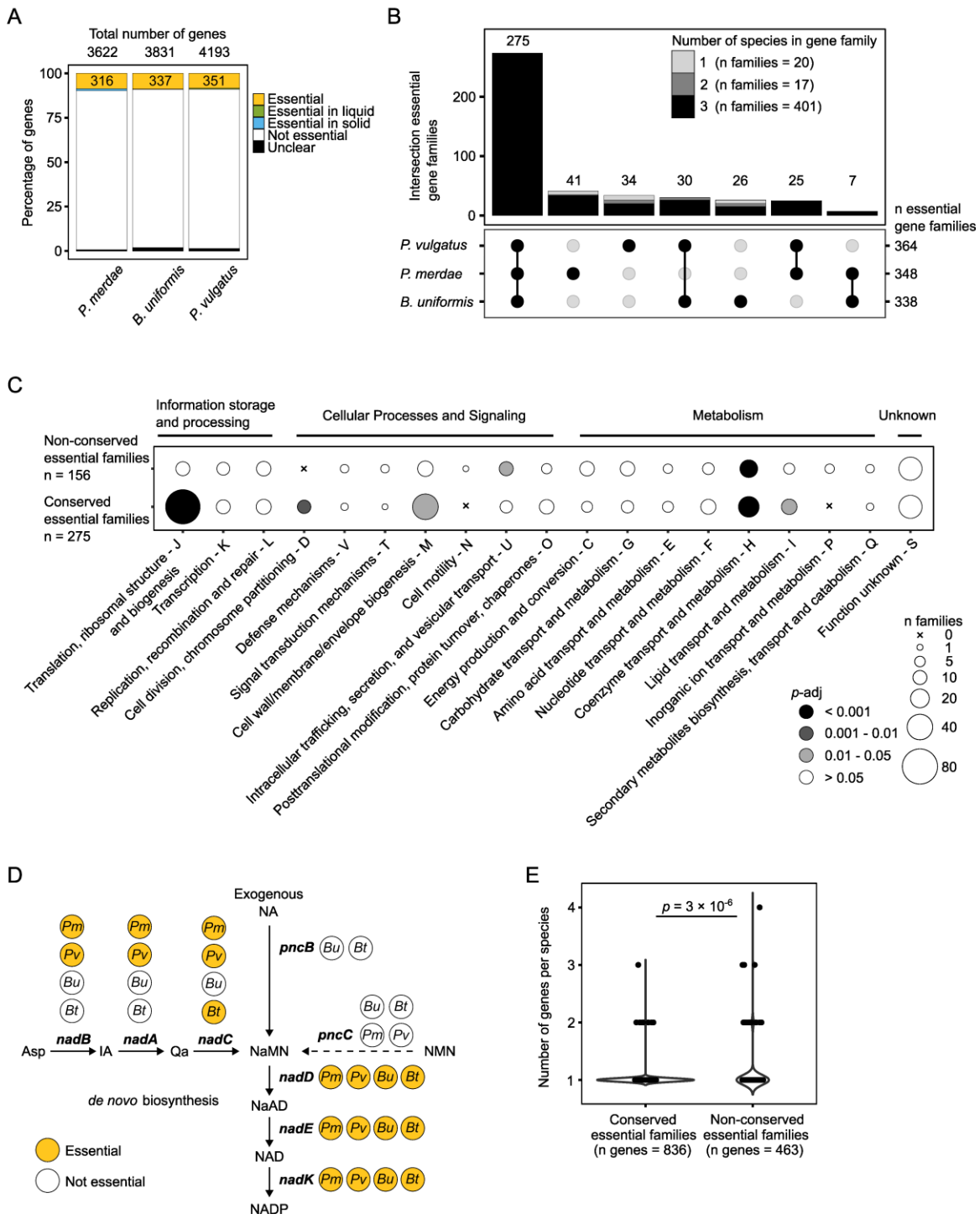

Fig 3. Gene essentiality across three species of Bacteroidales. A) Less than 10% of all genes are required for growth in rich media (mGAM) in all three species. At most, ~1.1% (*P. merdae*) of genes are only essential in either liquid or solid growth conditions. Essentiality calling is based on transposon insertion coverage per gene (Methods). **B)** Essential genes are largely conserved across the three genera with evidence of species-specific bypassing of gene essentiality. Over 60% of essential gene families are conserved across all three species, and over 75% in at least two species. Shown are essential gene families as defined by Cluster of Orthologous Groups (COGs) at the Bacteroidia taxonomic level (class). Bar shading reflects the number of tested species containing the COG. For example, among the 41 families that

are essential only in *P. merdae*, most also include non-essential orthologs in the other two species. **C)** Essential genes are enriched in core cellular processes. Functional enrichment analysis of conserved and non-conserved essential gene families from the three species using Cluster of Orthologous Groups (COG) functional categorization (indicated by capital letters). Dot shading represents the adjusted *p*-value (Benjamini–Hochberg correction) of a one-sided Fisher's exact test (testing for enrichment). Of the 163 non-conserved essential gene families, 7 lacked COG annotation and were excluded from the analysis. COG categories without essential gene families are not shown. **D)** The *de novo* pathway for NAD biosynthesis is essential in *P. merdae* and *P. vulgatus*, but not in *B. uniformis* and *B. thetaiotaomicron* (based on prior essential analysis data[21]), which encode a salvage pathway from exogenous nicotinic acid (NA). The dashed line marks another putative salvage pathway through *pncC,* yet this does not enable bypassing of essentiality. Asp: Aspartate; IA: iminoaspartate; Qa: quinolinic acid; NaMN: nicotinate mononucleotide; NaAD: nicotinate adenine dinucleotide; NMN, nicotinamide mononucleotide; NAD(P): nicotinamide adenine dinucleotide (phosphate). **E)** Non-conserved essential genes are more frequently found in higher copy numbers than conserved essential genes across the three genera. Therefore, redundancy is likely a common mechanism for bypassing essentiality. Shown are the number of genes within conserved essential families across all three species (n = 275) against those within non-conserved essential families (n = 163). Statistical significance was assessed using a two-sided Wilcoxon rank-sum test. For specific examples see Extended Data. Fig. 4D.

Figure 4

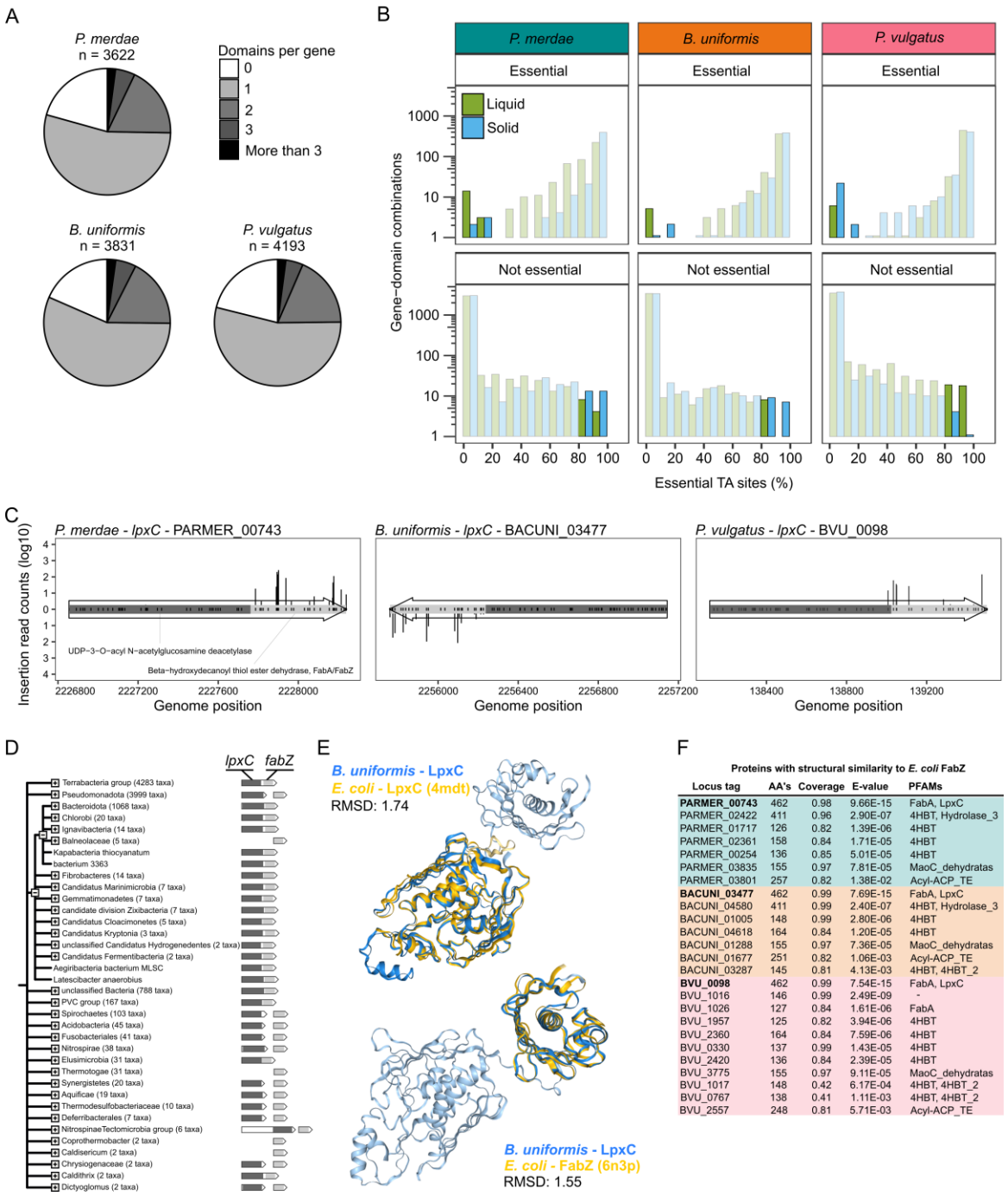

Locus tag	AA's	Coverage	E-value	PFAMs
PARMER_00743	462	0.98	9.66E-15	FabA, LpxC
PARMER_02422	411	0.96	2.90E-07	4HBT, Hydrolase_3
PARMER_01717	126	0.82	1.39E-06	4HBT
PARMER_02361	158	0.84	1.71E-05	4HBT
PARMER_00254	136	0.85	5.01E-05	4HBT
PARMER_03835	155	0.97	7.81E-05	MaoC_dehydratas
PARMER_03801	257	0.82	1.38E-02	Acyl-ACP_TE
BACUNI_03477	462	0.99	7.69E-15	FabA, LpxC
BACUNI_04580	411	0.99	2.40E-07	4HBT, Hydrolase_3
BACUNI_01005	148	0.99	2.80E-06	4HBT
BACUNI_04618	164	0.84	1.20E-05	4HBT
BACUNI_01288	155	0.97	7.36E-05	MaoC_dehydratas
BACUNI_01677	251	0.82	1.06E-03	Acyl-ACP_TE
BACUNI_03287	145	0.81	4.13E-03	4HBT, 4HBT_2
BVU_0098	462	0.99	7.54E-15	FabA, LpxC
BVU_1016	146	0.99	2.49E-09	-
BVU_1026	127	0.84	1.61E-06	FabA
BVU_1957	125	0.82	3.94E-06	4HBT
BVU_2360	164	0.84	7.59E-06	4HBT
BVU_0330	137	0.99	1.43E-05	4HBT
BVU_2420	136	0.84	2.39E-05	4HBT
BVU_3775	155	0.97	9.11E-05	MaoC_dehydratas
BVU_1017	148	0.42	6.17E-04	4HBT, 4HBT_2
BVU_0767	138	0.41	1.11E-03	4HBT, 4HBT_2
BVU_2557	248	0.81	5.71E-03	Acyl-ACP_TE

Fig. 4: Identification of essential protein domains with transposon mutant data. A) Most genes of the three species encode a single protein domain. Genes are grouped by the number of their encoded protein domains per species, according to domain identification using InterProScan. *N* indicates the total number of genes analyzed. **B)** Some essential and non-essential genes encode non-essential and essential protein domains. respectively. Plotted are domains with ≥10 TA sites from genes classified as essential or non-essential, binned by the fraction of TA sites predicted to be essential using the HMM method in TRANSIT (bin width = 10%). Highlighted bars indicate cases where domains and their host gene have contrasting essentiality: non-essential domains (<20% essential sites) within essential genes (top row) and essential domains (>80% essential sites) within non-essential genes (bottom row). **C)**

lpxC encodes two protein domains in Bacteroidales with only the one involved in lipid A biosynthesis being essential. The second domain encoding *fabZ* and involved in fatty acid biosynthesis tolerates insertions. Shown are the insertions and their read counts in the two domains of *lpxC* – domains shown in gray colors. Insertions are shown as vertical black bars. Gene arrows indicate coding direction. Transposon insertions into the forward genomic strand (+) are shown above the arrow, and insertions on the reverse strand (−) below. Black tick marks within the domain bar indicate TA sites. **D)** *lpxC* (dark gray) and *fabZ* (light gray) are fused in Bacteroidota, but appear as separate genes in different taxonomic groups of bacteria, including Pseudomonadota (formerly Proteobacteria). Taxonomic groups that show the fusion gene may include (limited) species in which the genes are separate, but the opposite does not occur. Figure is adapted from output generated by STRING-db version 12.0[110]. **E)** AlphaFold2 model of *B. uniformis* LpxC (BACUNI_03477) fusion protein (blue tones) superimposed on the crystal structures of either *E. coli* LpxC or FabZ (gold) using Foldseek. RMSD: Root Mean Square Deviation. **F)** Several proteins of *P. merdae* (PARMER), *B. uniformis* (BACUNI) and *P. vulgatus* (BVU) are predicted by Foldseek to fold similarly as *E. coli* FabZ chain A (PDB: 6n3p). Locus tags in bold are the *lpxC* genes shown in panel C. AA's: number of amino acid residues; Coverage: fraction of protein that aligned to *E. coli* FabZ; E-value: Expect-value; PFAMs: protein families to which the protein belongs. 4HBT: 4-hydroxybenzoyl-CoA thioesterase; Acyl-ACP_TE: acyl-acyl carrier protein (ACP) thioesterases (TE).

Figure 5

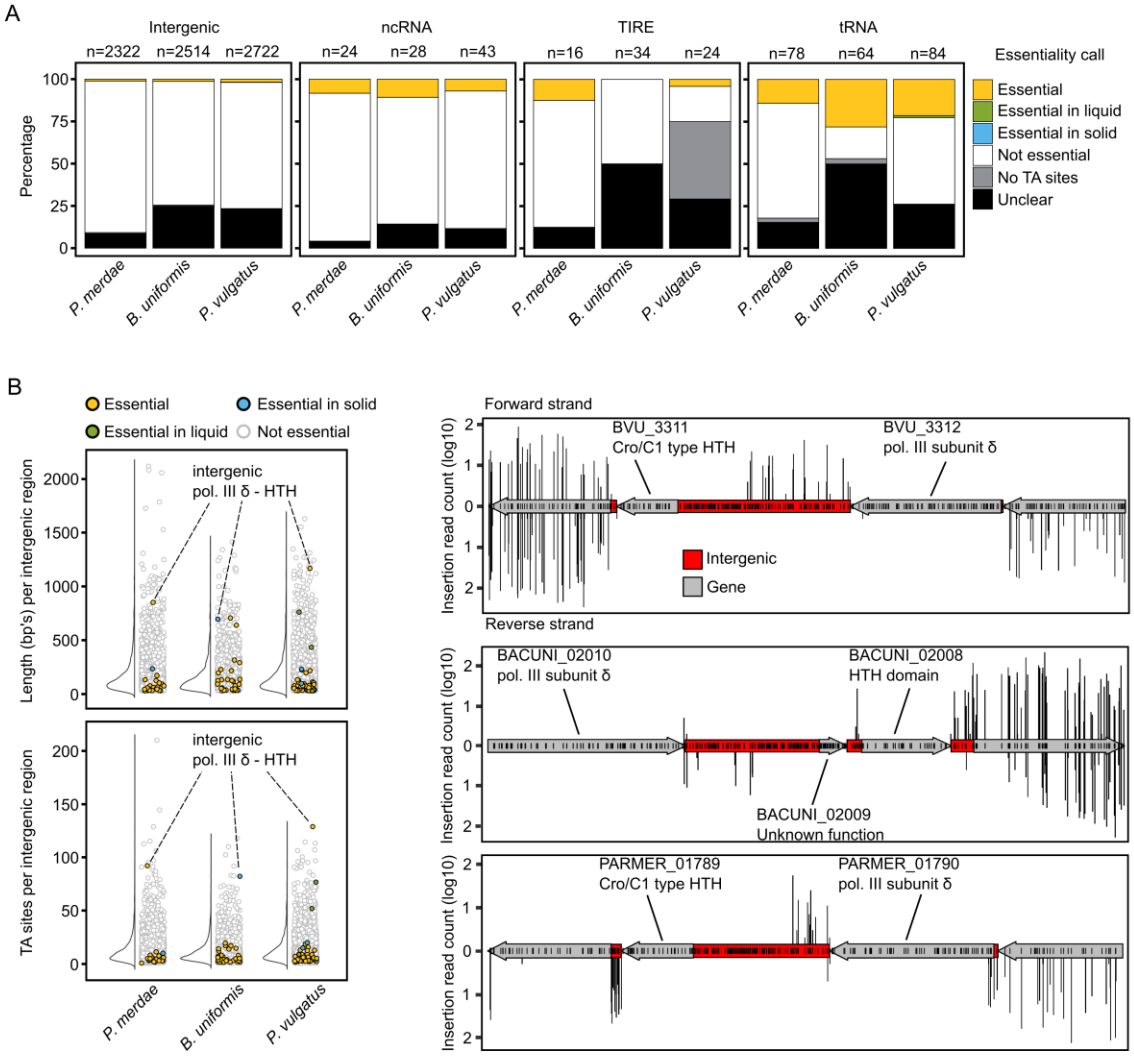

Fig. 5: Essentiality of non-protein-coding regions. **A**) Most non-protein-coding elements are not essential. Proportion of annotated intergenic regions, non-coding RNAs (ncRNAs), terminal inverted repeat elements (TIREs), and transfer RNAs (tRNAs) with essentiality calls across the three species. **B**) A long conserved essential intergenic region between the DNA polymerase III δ subunit and a putative helix-turn-helix (HTH) transcriptional regulator. Left panels: distribution of number of TA sites in intergenic regions across the three species (function of intergenic region length), color-coded by essentiality status. Intergenic regions with no TA sites or unclear essentiality are not shown. The conserved essential intergenic region between the DNA polymerase III δ subunit and a putative helix-turn-helix (HTH) transcriptional regulator shown in the right panel is marked. Right panel: transposon insertion profiles for intergenic regions (red) and genes (gray) in *P. vulgatus* (top), *B. uniformis* (middle), and *P. merdae* (bottom). Genes and transposon insertions are depicted as in Fig. 4C.

Figure 6

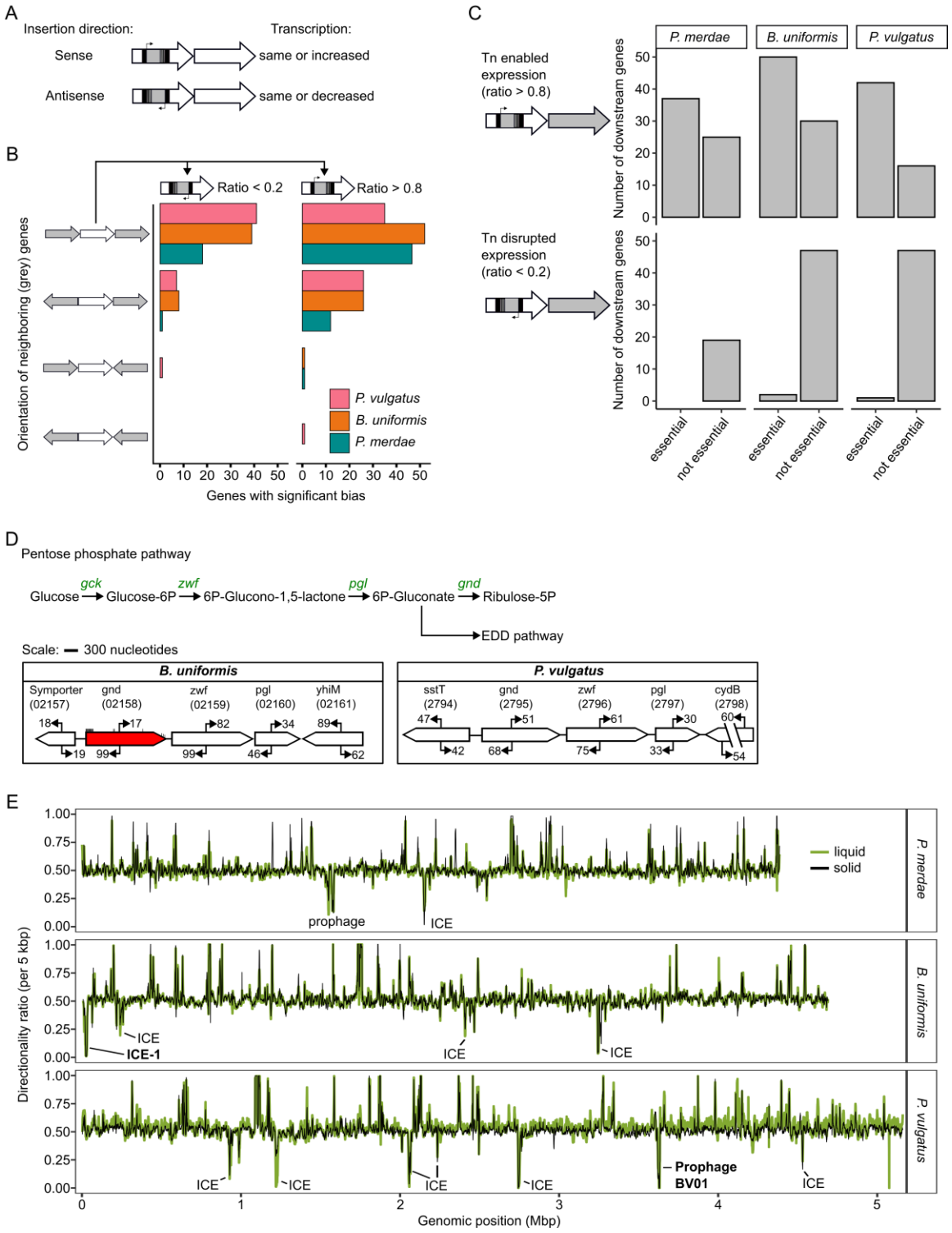

Fig. 6: Directionality bias in transposon insertions indicates functional relations between genes. A) Schematic of how insertion orientation may affect downstream transcription. **B)** Genes display directionality bias only when the downstream gene has the same orientation – operon effects. Number of significantly biased genes (two-sided binomial test, Benjamini–Hochberg adjusted $p < 0.01$) grouped by orientation of their immediate neighboring genes, across the three species. The directionality ratio is defined as the fraction of sense-strand insertions over all insertions in a given gene. **C)** Essential genes counter-

select antisense transposon insertions in upstream genes. Number of essential and non-essential genes downstream of significantly biased genes (binomial test, BH adjusted $p < 0.01$). **D)** Insertion bias in *gnd* suggests that production of the downstream pentose phosphate pathway genes is toxic in *B. uniformis*, but not in *P. vulgatus*. A partial pentose phosphate pathway map is shown. *gck*, glucokinase; *gnd*, 6-phosphogluconate dehydrogenase; *zwf*, glucose-6-phosphate 1-dehydrogenase; *pgl*, 6-phosphogluconolactonase; EDD, Entner–Doudoroff pathway. Arrows from the genes indicate the directionality and number of insertions summarized over the gene. *B. uniformis gnd* is highlighted in red showing a significant insertion bias (binomial test, BH adjusted $p < 0.01$, directionality ratio < 0.2). Insertions in B. *uniformis gnd* sense strand are shown as small tick marks indication mostly insertions at the edges of the gene. Genes are drawn to scale but intergenic regions are not. Locus tag identifiers (BACUNI or BVU) are indicated below gene names in parentheses. **E)** Mobile genetic elements are enriched in genes with insertion bias to avoid downstream gene expression. Genome-wide directionality ratios were calculated for coding genes in sliding windows of 5 kbps with 500 bp steps. Regions with strong bias frequently mapped to integrative and conjugative elements (ICEs) and prophages. Elements in bold are shown in detail in Extended Data Fig. 8. The line of the solid library is thinner than that of the liquid library to improve visualization.

1286 **Extended data with legends**
ED figure 1

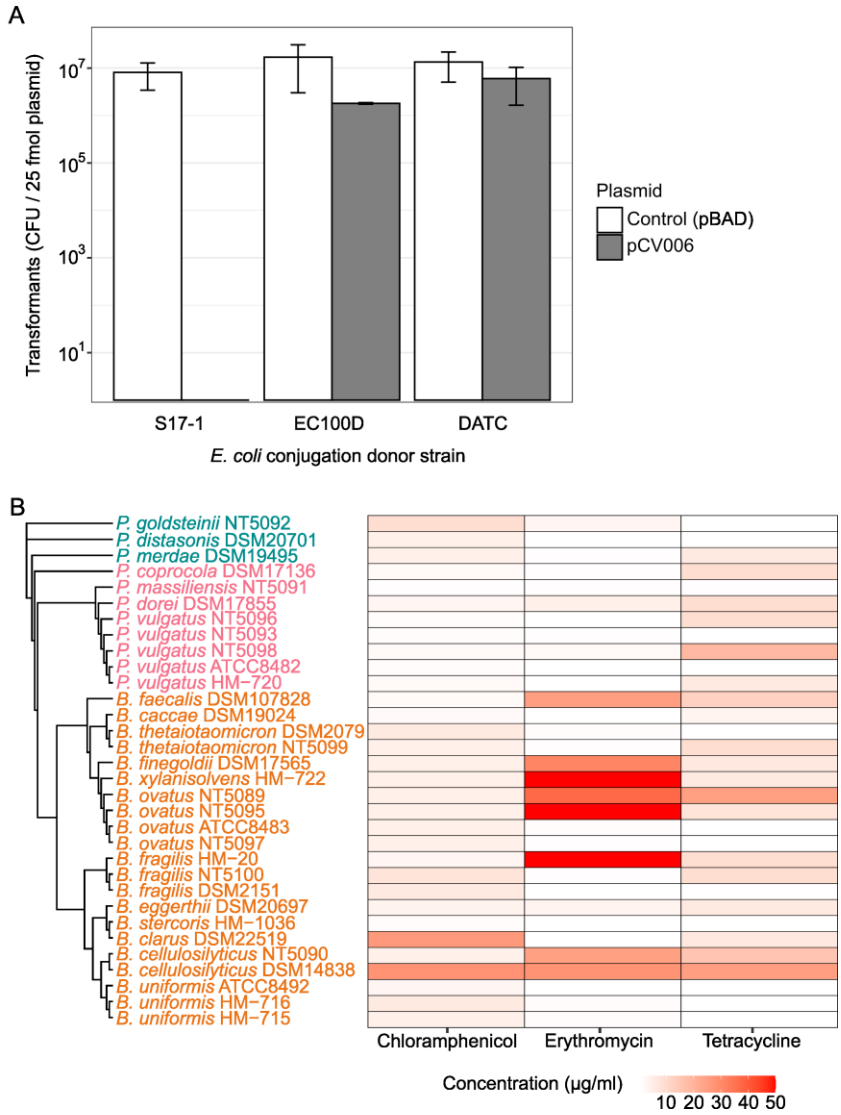

1287
1288 **Extended data Fig. 1: Transformation efficiency of *E. coli* DATC donor strain and**
1289 **antibiotic resistance profiles of Bacteroidales strains**. **A)** The *E. coli* cloning-conjugation
1290 donor strain DATC can be transformed with high efficiency. Transformation efficiency of the
1291 pCV006 transposon vector or a control plasmid (pBAD) into different strains of *E. coli* – shown
1292 as CFU of ~ 5 x 10^9 input cells per 25 fmol plasmid. Bars indicate the mean and SEM of three
1293 biological replicates. **B)** Antibiotic resistance among strains of diverse Bacteroidales species.
1294 Shown in red shade is the highest concentration of chloramphenicol, erythromycin and
1295 tetracycline (maximum concentration tested was 50 µg/ml) for which growth was observed
1296 among 32 strains of *Parabacteroides* (green), *Phocaeicola* (pink) and *Bacteroides* (orange)
1297 species. Values indicate the mean of two biological replicates. Strains are grouped by
1298 phylogeny according to a neighbor-joining tree build on whole genome average nucleotide
1299 identity approximated with Mash version 2.3[109].
1300

ED Figure 2

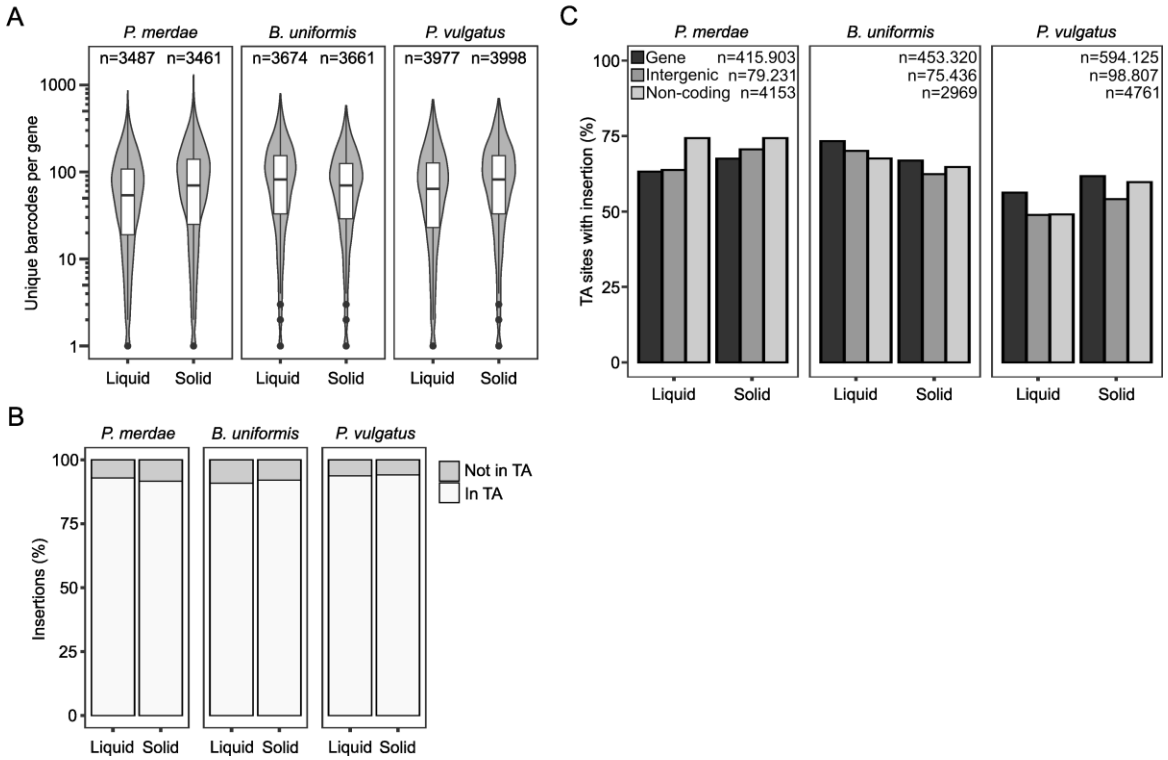

Extended data Fig. 2: Barcode coverage and genomic distribution of insertions across transposon libraries. A) Almost all genes in the 6 libraries are represented by multiple unique barcodes. *N* indicates number of genes analyzed. Boxplots show the distribution of the number of unique barcodes per gene in each transposon library. The center line represents the median; box limits indicate the first and third quartiles; whiskers extend to 1.5 x the interquartile range; and points represent outliers. **B)** Percentage of insertions at TA dinucleotide versus any other site per library. **C)** Percentage of TA dinucleotide sites with insertions in genes, annotated non-coding features and intergenic regions. Inset numbers indicate the total number of TA sites per feature in each species.

ED. Figure 3

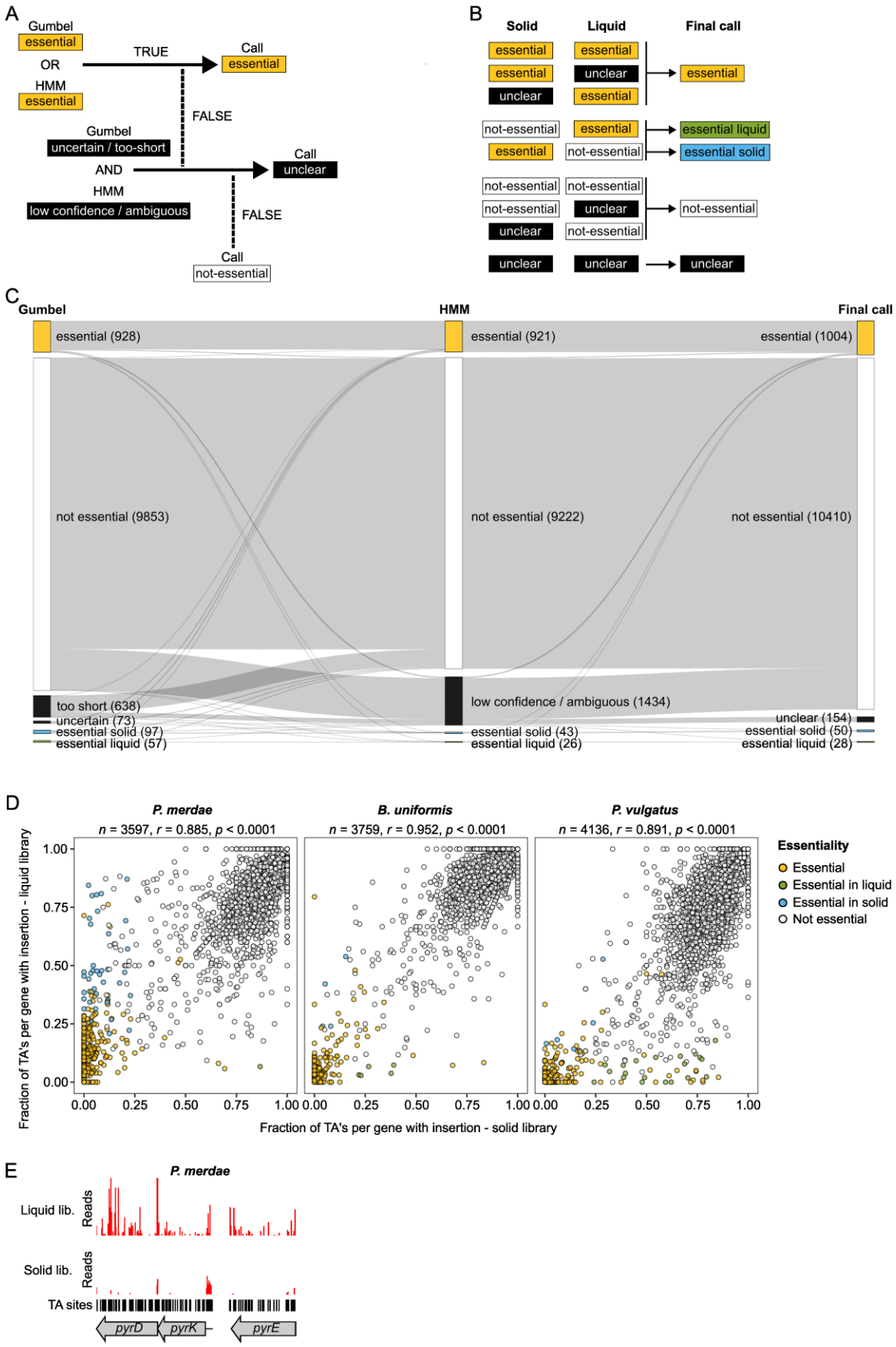

Extended data Fig. 3: Gene essentiality calling between solid and liquid libraries. A)

Logic used to consolidate essentiality calls from TRANSIT's Gumbel and HMM methods post analysis. **B)** Logic used to consolidate calls from libraries grown on solid and liquid media to create the final essentiality call. **C)** Flow diagram illustrating the combined number of genes from the three species, their essentiality call by the Gumbel and HMM methods and how the consolidation between these two methods yields the final essentiality call (Supplementary table 1). **D)** Essentiality calls strongly agree between solid and liquid grown libraries. Shown are the fraction of TA dinucleotide sites per gene with transposon insertions in solid (x axis) versus liquid (y axis) libraries for the three species. n = number of genes, r = Pearson correlation coefficient, p = p-value (two-sided). **E)** Representative TRANSIT insertion plots of *P. merdae pyr* genes from pyrimidine metabolism that are essential in liquid growth conditions (in contrast to solid conditions), possibly due to complementation of auxotrophies in the pooled library.

ED Figure 4

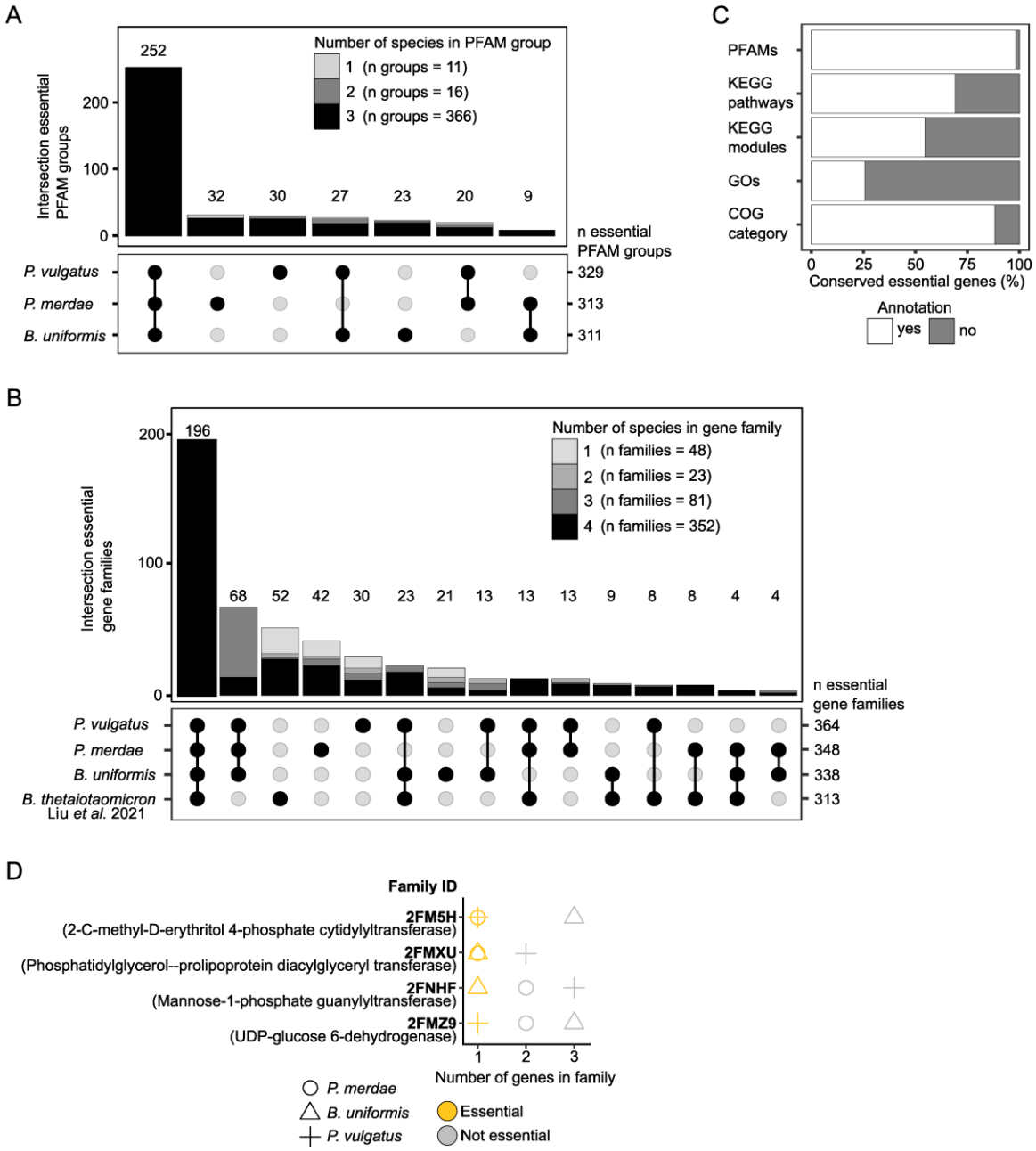

Extended data Fig. 4: Conservation, annotation, and copy number shape essential gene families in Bacteroidales. A) Conservation and species-specificity of gene essentiality is preserved when genes are grouped by their annotated PFAMs instead of eggNOG COGs – plotted as in Fig. 3B. **B)** Addition of *B. thetaiotaomicron* essential genes from Liu *et al*., 2021[21] largely preserves the core essentialome of members of the Bacteroidales. Shown are essential gene families as defined by Cluster of Orthologous Groups (COGs) at the Bacteroidia (class) taxonomic level – plotted as in Fig. 3B. **C)** Most conserved essential genes have a functional annotation, yet some lack any annotation from the indicated functional categorization resources. Shown is the percentage of genes (n = 836) that are in the 275 conserved essential gene families (some families have more than one gene per species) from Fig. 3B. **D)** Essentiality depends on gene copy number. Shown are examples of Bacteroidia taxonomy level (class) eggNOG gene families in which single-copy genes are essential, while in species for which the same family has additional members, all are not essential.

ED figure 5

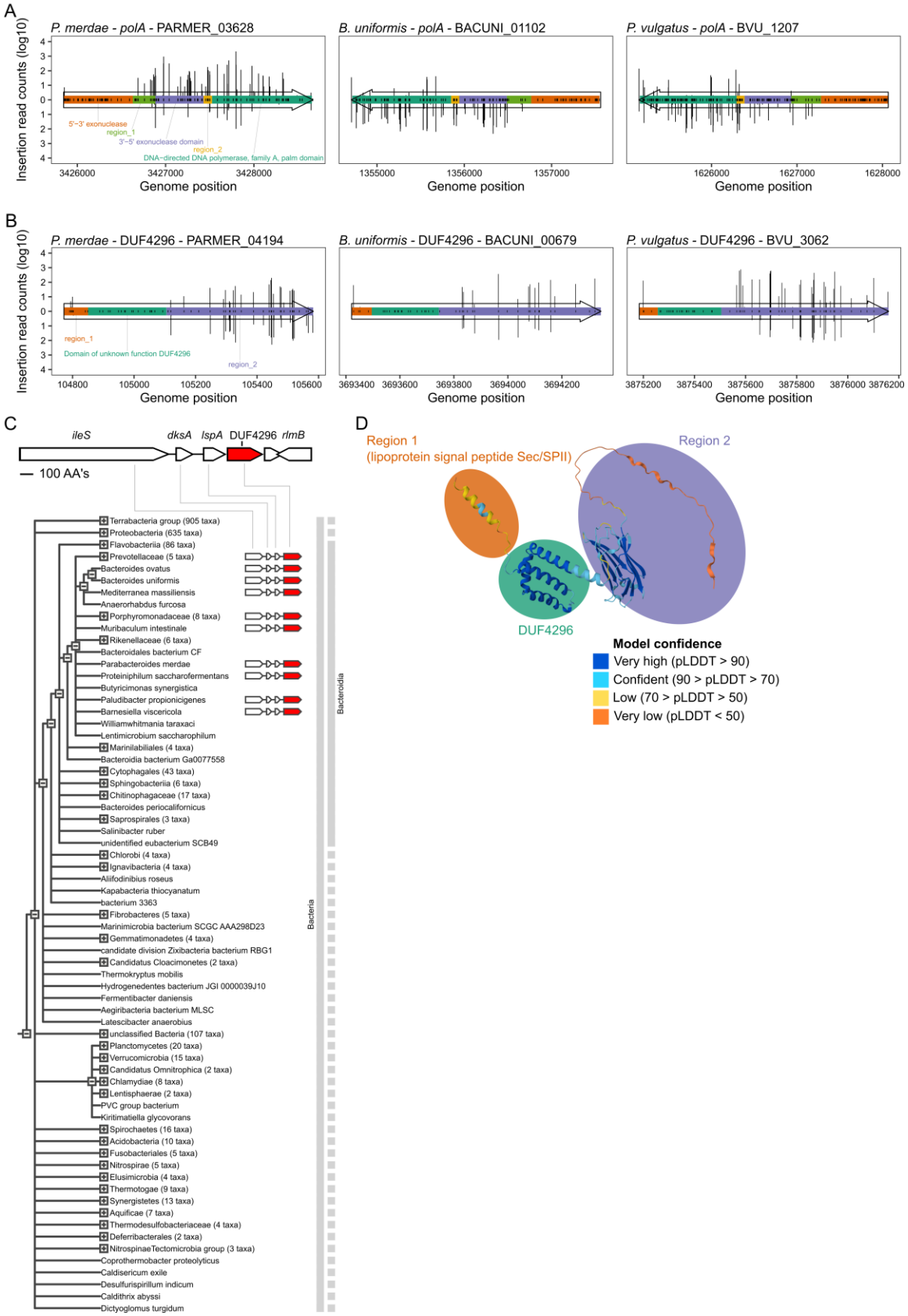

Extended data Fig. 5: Examples of sub-gene essentiality of encoded protein domains. A) Only the 5' to 3' exonuclease domain of DNA polymerase I (*polA*) is essential. Shown are insertions and their read counts in the different domains in *polA* (color-coded and denoted in

inset). Gene arrows indicate coding direction (5′→3′, sense strand). Transposon insertions into the forward genomic strand (+) are shown above the arrow, and insertions on the reverse strand (−) below. Colors within the arrow indicate the different domains and regions. Black tick marks within the arrow indicate TA sites. **B)** Insertion plot as in A of a conserved, Bacteroidota-specific uncharacterized gene with an essential domain of unknown function (DUF4296). Insertions are not tolerated within the DUF4296, but are frequent within the two adjacent regions of the gene. **C)** Presence and genomic neighbors of the uncharacterized gene with DUF4296 across different taxonomic groups of bacteria (visualization is adapted from output generated by STRING-db[110]). **D)** Predicted structure (pTM score = 0.48) of the *P. vulgatus* DUF4296 encoding gene (BVU_3062) obtained by Alphafold3[111]. Colors indicate the model confidence score pLDDT (predicted local distance difference test).

ED figure 6

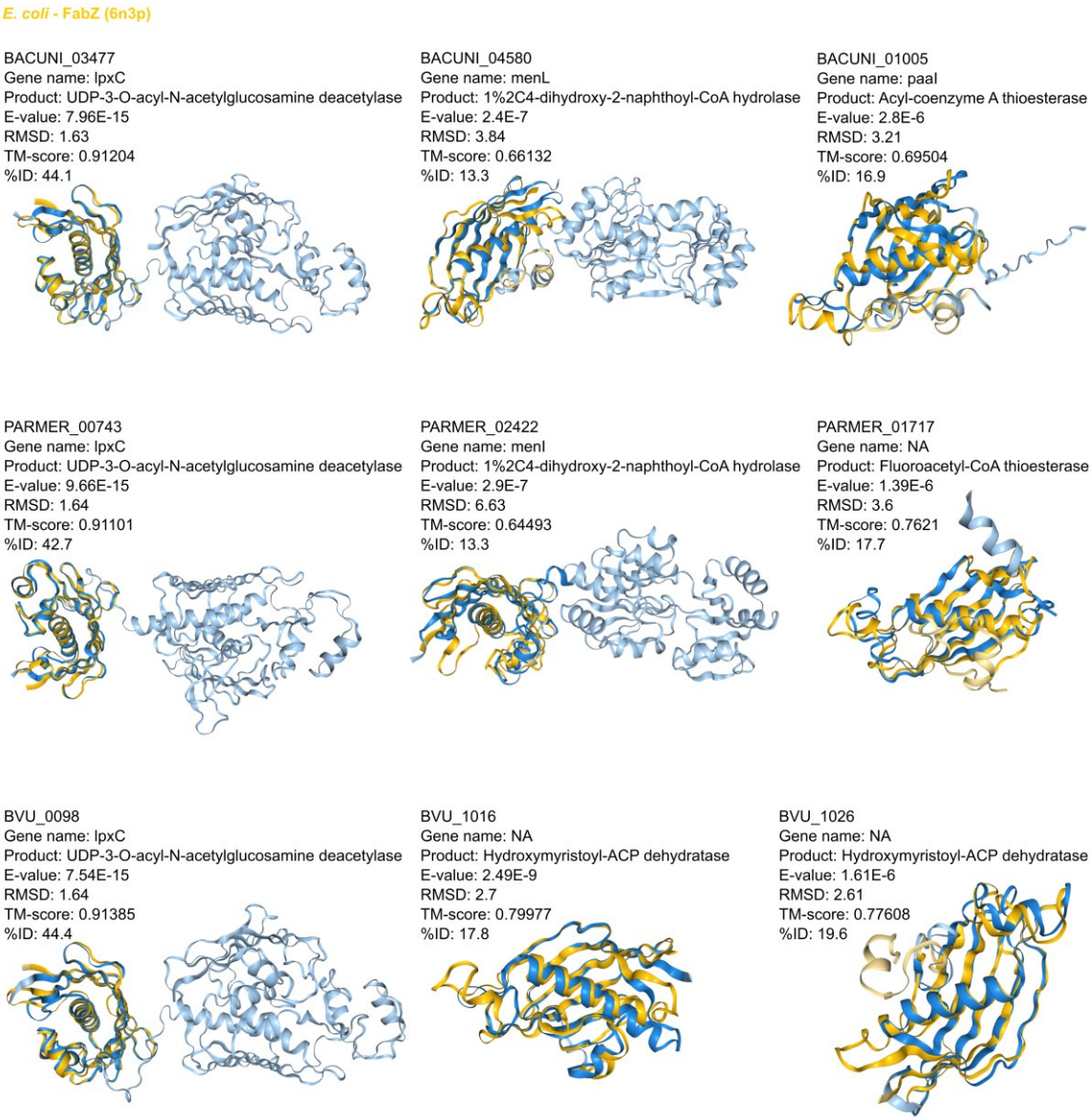

Extended data Fig. 6: Structural similarity of Bacteroidales proteins to *E. coli* FabZ. Shown are the top three proteins of *P. merdae*, *B. uniformis* and *P. vulgatus* that are predicted by Foldseek[73] to have the highest similarity (lowest E-value, Fig. 4F) to *E. coli* FabZ (in gold). RMSD: Root Mean Square Deviation. TM: Template Modeling score. %ID: percentage of identical amino acid residues in the alignment.

ED figure 7

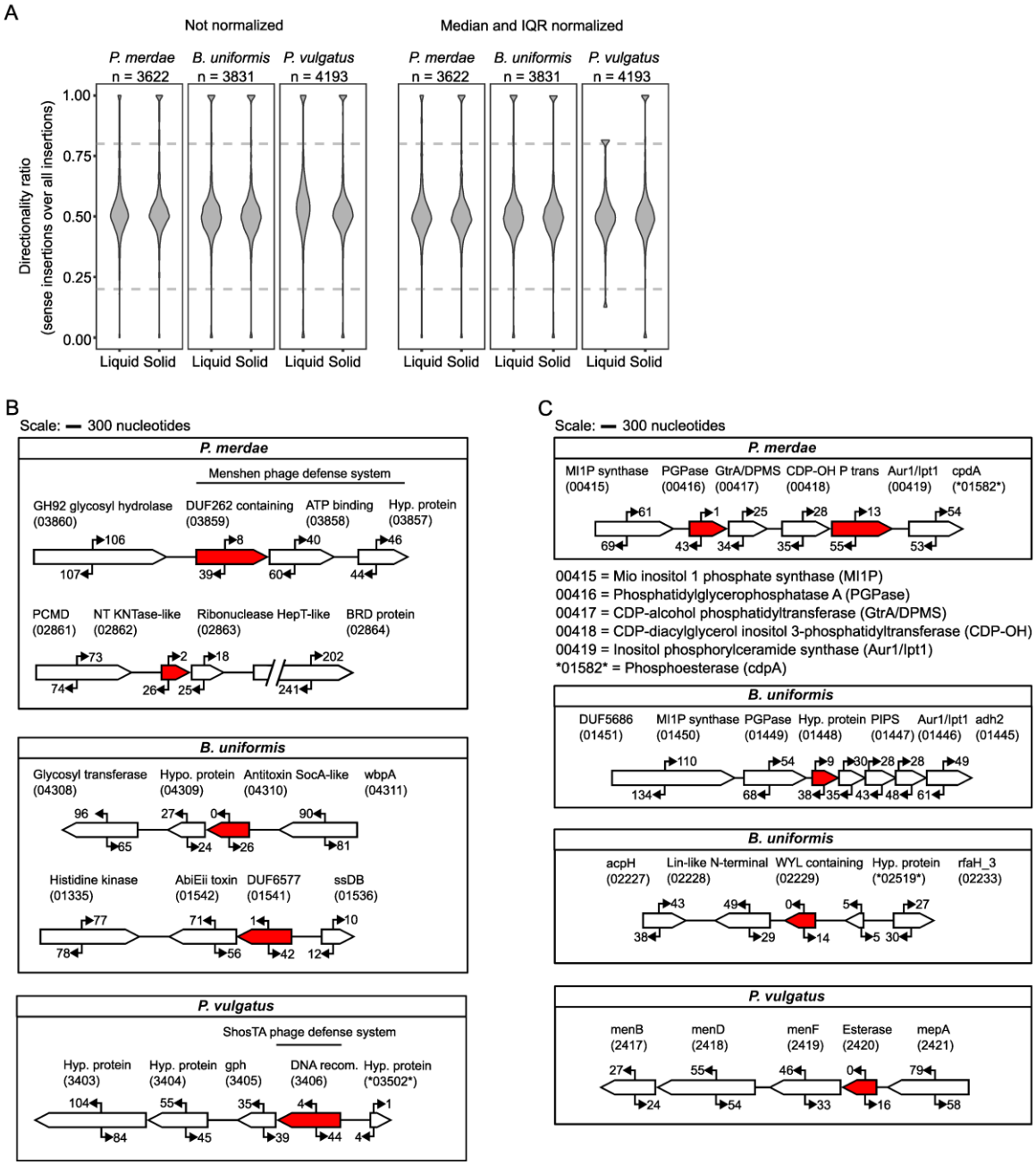

Extended Data Fig. 7: Directionality bias of transposon insertions. A) Some genes show strong strand bias, either favoring sense insertions (ratio > 0.8) that permit downstream expression or antisense insertions (ratio < 0.2) that suppress it. Violin plots show the distribution of directionality ratios (fraction of sense-strand insertions per gene) across all libraries, before and after median/IQR normalization. Dashed grey lines indicate 0.8 and 0.2 thresholds. **B–C)** Examples of biased genes in toxin–antitoxin and phage defense systems (B), and in metabolic pathways (C). Arrows represent the orientation and number of insertions per gene. Significantly biased genes (two-sided binomial test, Benjamini–Hochberg adjusted $p < 0.01$; directionality ratio < 0.2) are shown in red. Genes (but not intergenic regions) are drawn to scale (scale bar: 300 nt). Numbers below gene names in parentheses indicate locus tags (PARMER, BACUNI, BVU). Numbers marked with asterisks indicate genes without canonical locus tags; these instead carry PM_ATCC43184, BU_ATCC8492, or PV_ATCC8482 identifiers introduced in this study (Supplementary table 1).

ED figure 8

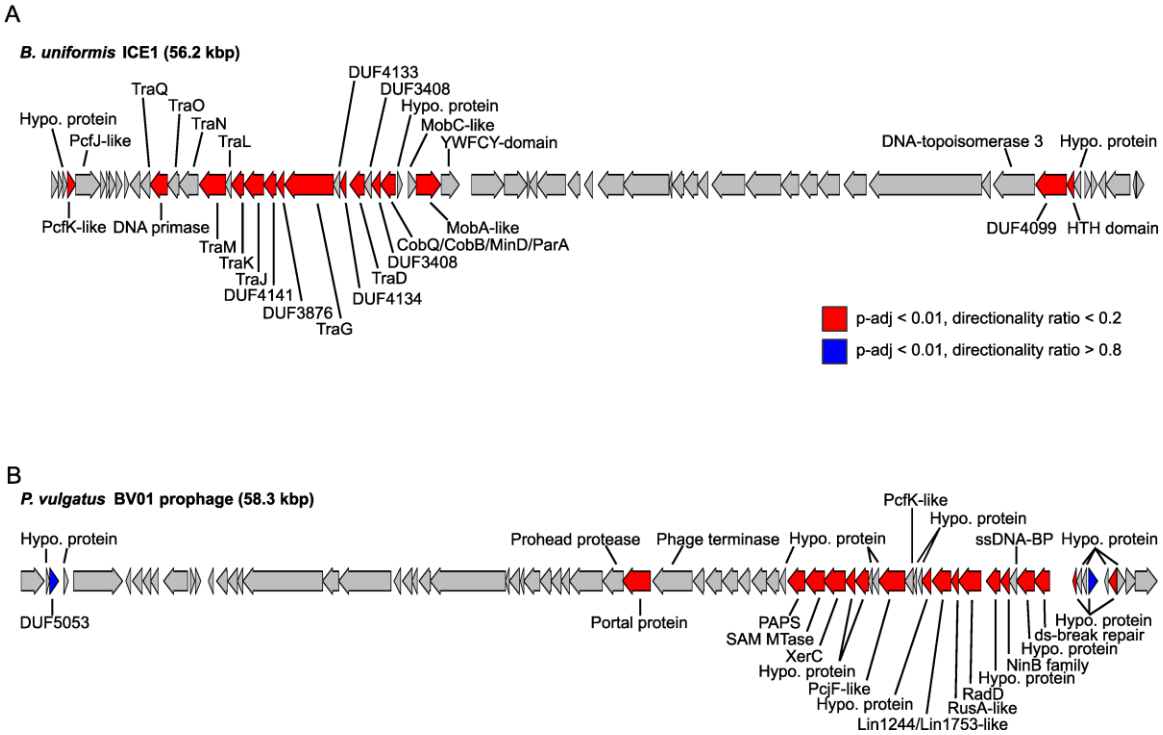

Extended Data Fig. 8: Clusters of directionality-biased genes in mobile genetic elements. A) An integrative and conjugative element (ICE) in *B. uniformis* contains multiple genes biased against downstream expression. **B)** The *P. vulgatus* prophage BV01 contains multiple genes near one end that are similarly biased to avoid mostly downstream gene expression. In both panels significantly biased genes are shown in red (antisense insertions; directionality ratio < 0.2) and blue (sense insertions; directionality ratio > 0.8) – significance assessed by two-sided binomial test, Benjamini–Hochberg adjusted $p < 0.01$.

Supplementary material

Supplementary figure 1

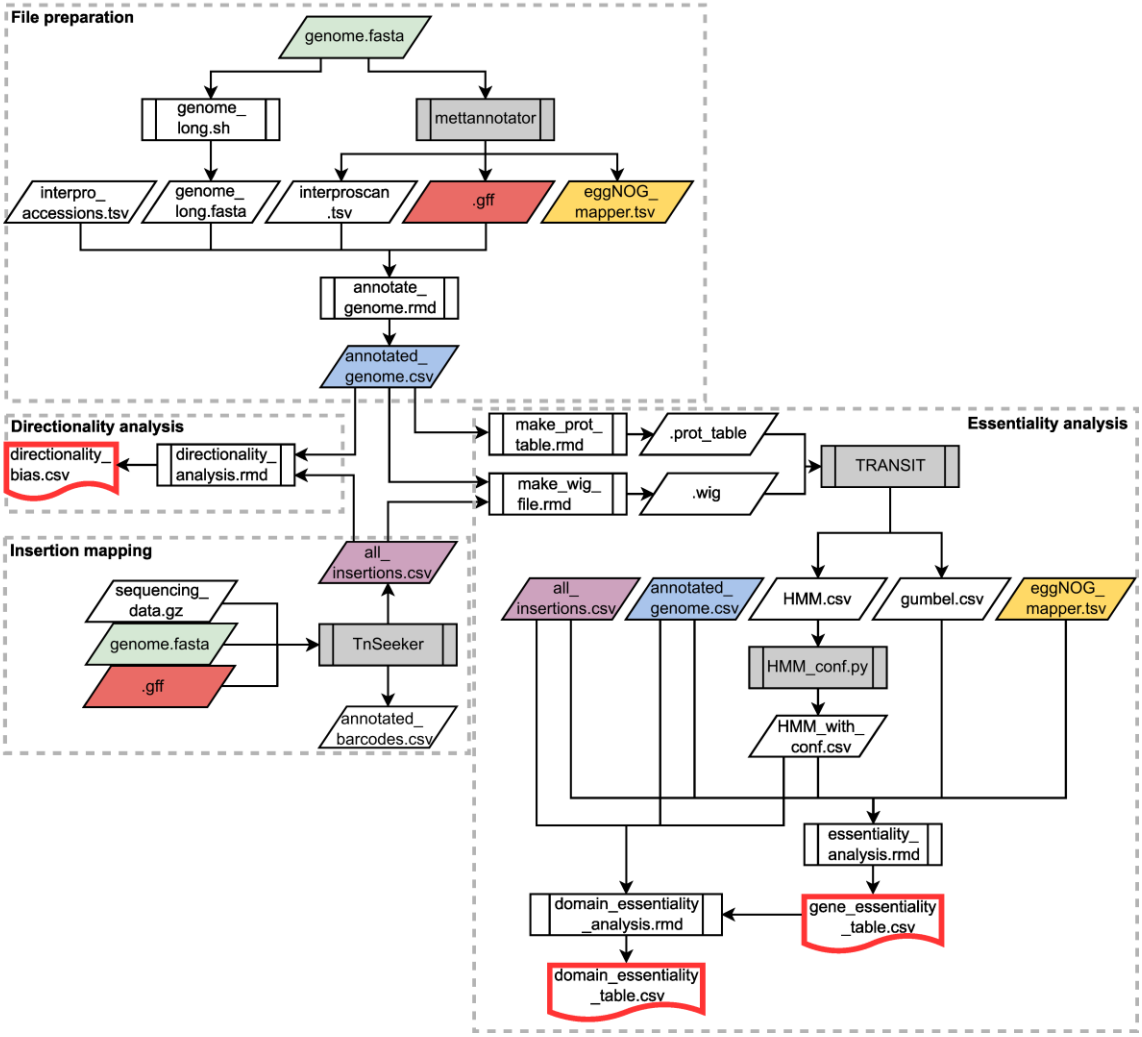

Supplementary Fig. 1: Inputs, outputs and softwares used to perform the functional genomics analyses. Flowchart depicting the input and output files and softwares and scripts for the functional genomics analyses. Recurrent files are color coded. Scripts for processes in white background are provided with this work and can be downloaded from https://git.embl.org/grp-typas/transposon_toolkit. Processes in gray background are described elsewhere, see Methods. Output files outlined in red are the final files for essentiality, domain essentiality and directionality data.

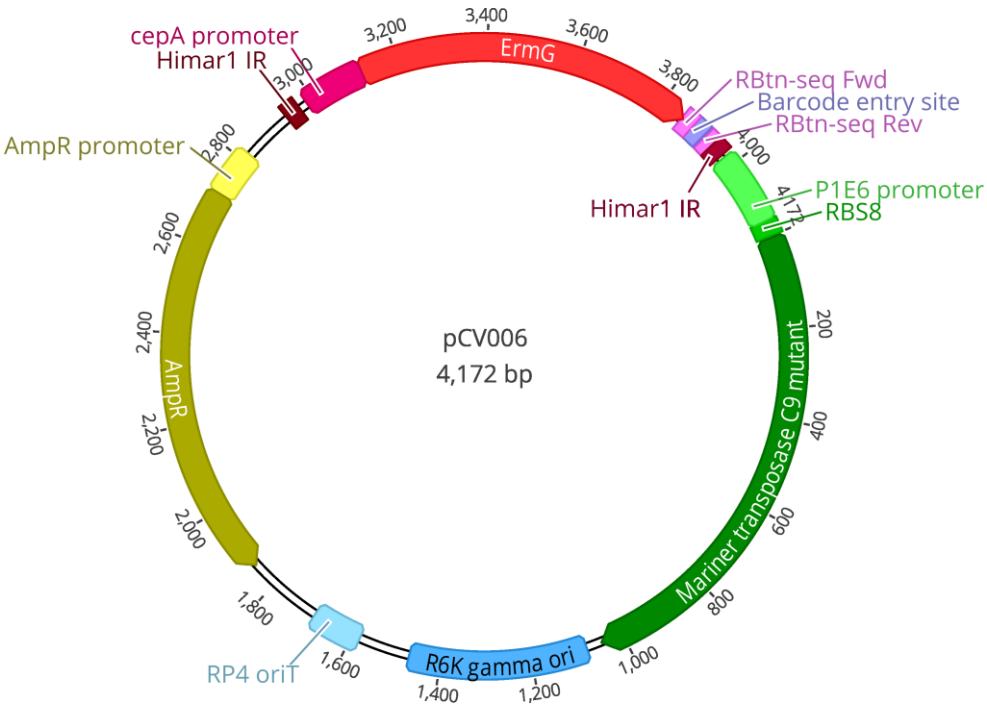

Supplementary file 1: Plasmid features and sequence

```
FEATURES             Location/Qualifiers
     misc_feature    1..1047
                     /label="Mariner transposase C9 mutant"
     rep_origin      1080..1468
                     /label="R6K gamma ori"
     oriT            1583..1692
                     /label="RP4 oriT"
     CDS             complement(1856..2716)
                     /label="AmpR"
     promoter        2717..2821
                     /label="AmpR promoter"
     misc_feature    2935..2966
                     /label="Himar1 IR"
     misc_feature    2987..3122
                     /label="cepA promoter"
     misc_feature    3123..3857
                     /label="ErmG"
     misc_feature    3854..3880
                     /label="BarSeq Fwd"
     misc_feature    3878..3911
                     /label="Barcode entry site"
     misc_feature    3915..3940
                     /label="BarSeq Rev"
     misc_feature    3926..3957
                     /label="Himar1 IR"
     regulatory      3976..4139
                     /label="P1E6 promoter"
     regulatory      4140..4172
                     /label="RBS8"
ORIGIN
        1 atggaaaaaa aggaatttcg tgttttgata aaatactgtt ttctgaaggg aaaaaataca
       61 gtggaagcaa aaacttggct tgataatgag tttccggact ctgccccagg gaaatcaaca
      121 ataattgatt ggtatgcaaa attcaagcgt ggtgaaatga gcacggagga cggtgaacgc
      181 agtggacgcc cgaaagaggt ggttaccgac gaaaacatca aaaaaatcca caaaatgatt
      241 ttgaatgacc gtaaaatgaa gttgatcgag atagcagagg ccttaaagat atcaaaggaa
      301 cgtgttggtc atatcattca tcaatatttg gatatgcgga agctctgtgc gaaatgggtg
      361 ccgcgcgagc tcacatttga ccaaaaacaa cgacgtgttg atgattctaa gcggtgtttg
```

```
1436    421 cagctgttaa ctcgtaatac acccgagttt ttccgtcgat atgtgacaat ggatgaaaca
1437    481 tggctccatc actacactcc tgagtccaat cgacagtcgg ctgagtggac agcgaccggt
1438    541 gaaccatctc cgaagcgtgg aaagactcaa aagtccgctg gcaaagtaat ggcctctgtt
1439    601 ttttgggatg cgcatggaat aatttttatc gattatcttg agaagggaaa aaccatcaac
1440    661 agtgactatt atatggcgtt attggagcgt ttgaaggtcg aaatcgcggc aaaacggccc
1441    721 cacatgaaga agaaaaaagt gttgttccac caagacaacg caccgtgcca caagtcattg
1442    781 agaacgatgg caaaaattca tgaattgggc ttcgaattgc ttccccaccc gccgtattct
1443    841 ccagatctgg cccccagcga ctttttcttg ttctcagacc tcaaaaggat gctcgcaggg
1444    901 aaaaaatttg gctgcaatga agaggtgatc gccgaaactg aggcctattt tgaggcaaaa
1445    961 ccgaaggagt actaccaaaa tggtatcaaa aaattggaag gtcgttataa tcgttgtatc
1446   1021 gctcttgaag ggaactatgt tgaataagcg gccgccaccg cggtggaggg gaattcccat
1447   1081 gtcagccgtt aagtgttcct gtgtcactca aaattgcttt gagaggctct aagggcttct
1448   1141 cagtgcgtta catccctggc ttgttgtcca caaccgttaa accttaaaag ctttaaaagc
1449   1201 cttatatatt ctttttttc ttataaaact taaaacctta gaggctattt aagttgctga
1450   1261 tttatattaa ttttattgtt caaacatgag agcttagtac gtgaaacatg agagcttagt
1451   1321 acgttagcca tgagagctta gtacgttagc catgagggtt tagttcgtta aacatgagag
1452   1381 cttagtacgt taaacatgag agcttagtac gtgaaacatg agagcttagt acgtactatc
1453   1441 aacaggttga actgctgatc ttcagatcct ctacgccgga cgcatcgtgg ccggatcaat
1454   1501 tccgtgatag gtgggctgcc cttcctggtt ggcttggttt catcagccat ccgcttgccc
1455   1561 tcatctgtta cgccggcggt agccggccag cctcgcagag caggattccc gttgagcacc
1456   1621 gccaggtgcg aataagggac agtgaagaag gaacacccgc tcgcgggtgg gcctacttca
1457   1681 cctatcctgc ccggctgacg ccgttggata caccaaggaa agtctacacg aaccctttgg
1458   1741 caaaatcctg tatatcgtgc gaaaaaggat ggatataccg aaaaaatcgc tataatgacc
1459   1801 ccgaagcagg gttatgcagc ggaaaacgga attgatcccc ctcgaattga cgcgttacc
1460   1861 aatgcttaat cagtgaggca cctatctcag cgatctgtct atttcgttca tccatagttg
1461   1921 cctgactccc cgtcgtgtag ataactacga tacgggaggg cttaccatct ggccccagtg
1462   1981 ctgcaatgat accgcgagac ccacgctcac cggctccaga tttatcagca ataaaccagc
1463   2041 cagccggaag ggccgagcgc agaagtggtc ctgcaacttt atccgcctcc atccagtcta
1464   2101 ttaattgttg ccgggaagct agagtaagta gttcgccagt taatagtttg cgcaacgttg
1465   2161 ttgccattgc tacaggcatc gtggtgtcac gctcgtcgtt tggtatggct tcattcagct
1466   2221 ccggttccca acgatcaagg cgagttacat gatcccccat gttgtgcaaa aaagcggtta
1467   2281 gctccttcgg tcctccgatc gttgtcagaa gtaagttggc cgcagtgtta tcactcatgg
1468   2341 ttatggcagc actgcataat tctcttactg tcatgccatc cgtaagatgc ttttctgtga
1469   2401 ctggtgagta ctcaaccaag tcattctgag aatagtgtat gcggcgaccg agttgctctt
1470   2461 gcccggcgtc aatacgggat aataccgcgc cacatagcag aactttaaaa gtgctcatca
1471   2521 ttggaaaacg ttcttcgggg cgaaaactct caaggatctt accgctgttg agatccagtt
1472   2581 cgatgtaacc cactcgtgca cccaactgat cttcagcatc ttttactttc accagcgttt
1473   2641 ctgggtgagc aaaaacagga aggcaaaatg ccgcaaaaaa gggaataagg gcgacacgga
1474   2701 aatgttgaat actcatactc ttccttttc aatattattg aagcatttat cagggttatt
1475   2761 gtctcatgag cggatacata tttgaatgta tttagaaaaa taaacaaata ggggttccgc
1476   2821 gcacatttcc ccgaaaagtg ccacctgacg tctaagaaac cattattatc atgacattaa
1477   2881 cctataaaaa taggcgtatc acgaggccct ttcgtcacgc gtcctcggta cctaacaggt
1478   2941 tggatgataa gtccccggtc ttcgtagata aaacgaaagg ctcagtaaag agttaaggaa
1479   3001 agtgaagcat cttcgatgct ggagtgggat atactaaatt acctaaaaaa gtggcgcaca
1480   3061 aatttgcgcg ccacaattat tattcatacc tttgtggacc gtattacaaa gaacccaatc
1481   3121 atatgaacaa agtaaatata aaagatagtc aaaattttat tacttcaaaa tatcacatag
1482   3181 aaaaaataat gaattgcata agtttagatg aaaaagataa catctttgaa ataggtgcag
1483   3241 ggaaaggtca ttttactgct ggattggtaa agagatgtaa ttttgtaacg gcgatagaaa
1484   3301 ttgattctaa attatgtgag gtaactcgta ataagctctt aaattatcct aactatcaaa
1485   3361 tagtaaatga tgatatactg aaatttacat ttcctagcca caatccatat aaaatatttg
1486   3421 gcagcatacc ttacaacata agcacaaata taattcgaaa aattgttttt gaaagttcag
1487   3481 ccacaataag ttatttaata gtggaatatg gttttgctaa aatgttatta gatacaaaca
1488   3541 gatcactagc attgctgtta atggcagagg tagatatttc tatattagca aaaattccta
1489   3601 ggtattattt ccatccaaaa cctaaagtgg atagcacatt aattgtatta aaaagaaagc
1490   3661 cagcaaaaat ggcatttaaa gagagaaaaa aatatgaaac ttttgtaatg aaatgggtta
1491   3721 acaaagagta cgaaaaactg tttacaaaaa atcaatttaa taaagcttta aaacatgcga
1492   3781 gaatatatga tataaacaat attagtttcg aacaatttgt atcgctattt aatagttata
1493   3841 aaatatttaa cggctaactg cagggatgtc cacgaggtgt atgagacgtc agaattggtt
1494   3901 aattcgtctc tcagaattgg gagtctacga agaccgggga cttatcatcc aacctgttag
1495   3961 aaaggcgatg aaagagataa aacgaaaggc tcagtcgaaa gactgggcct ttcgttttac
1496   4021 aattgggcta cctttttttt gttttgtttg caatggttaa tctattgtta aaatttaaag
```

```
     4081 tttcacttga actttcaaat aatgttctta tatttgcagt gtcgaaagaa acaaagtagg
     4141 actgatcgtc catcaattta aaatttaaaa ta
```

RBTnSeq amplicon

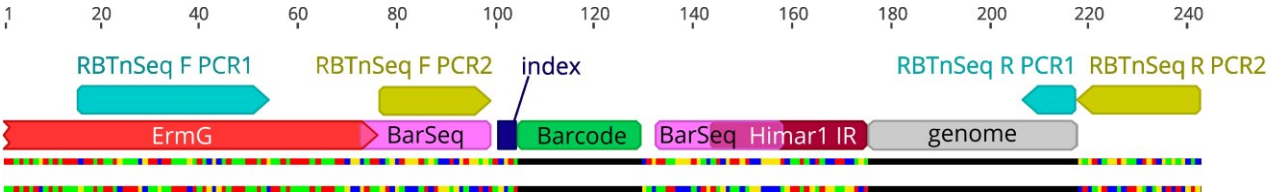


```
FEATURES             Location/Qualifiers
     misc_feature    <1..76
                     /label="ErmG"
     misc_feature    16..54
                     /label="RBTnSeq F PCR1"
     misc_feature    73..99
                     /label="BarSeq Fwd"
     misc_feature    77..99
                     /label="RBTnSeq F PCR2"
     misc_feature    101..104
                     /label="index"
     misc_feature    105..129
                     /label="Barcode"
     misc_feature    133..158
                     /label="BarSeq Rev"
     misc_feature    144..175
                     /label="Himar1 IR"
     misc_feature    176..242
                     /label="genome"
     misc_feature    complement(232..242)
                     /label="RBTnSeq R PCR1"
     misc_feature    complement(243..267)
                     /label="RBTnSeq R PCR2"
ORIGIN
        1 aatatatgat ataaacaata ttagtttcga acaatttgta tcgctattta atagttataa
       61 aatatttaac ggctaactgc agggatgtcc acgaggtgta cgatnnnnnn nnnnnnnnnn
      121 nnnnnnnnnc agaattggga gtctacgaag accggggact tatcatccaa cctgtnnnnn
      181 nnnnnnnnnn nnnnnnnnnn nnnnnnnnnn nnnnnnnnnn nnnnnnnnnn nnnnnnnnnn
      241 nngtgactgg agttcagacg tgtgctc
```